

1986

# Etching radiation treated polyimide films in O<sub>2</sub>/ NF<sub>3</sub> and O<sub>2</sub>/CF<sub>4</sub> plasmas

Eric P. Dibble  
*Lehigh University*

Follow this and additional works at: <https://preserve.lehigh.edu/etd>



Part of the [Manufacturing Commons](#)

---

## Recommended Citation

Dibble, Eric P., "Etching radiation treated polyimide films in O<sub>2</sub>/NF<sub>3</sub> and O<sub>2</sub>/CF<sub>4</sub> plasmas" (1986). *Theses and Dissertations*. 4997.  
<https://preserve.lehigh.edu/etd/4997>

This Thesis is brought to you for free and open access by Lehigh Preserve. It has been accepted for inclusion in Theses and Dissertations by an authorized administrator of Lehigh Preserve. For more information, please contact [preserve@lehigh.edu](mailto:preserve@lehigh.edu).

Etching Radiation Treated Polyimide Films

in  $O_2/NF_3$  and  $O_2/CF_4$  Plasmas

by

Eric P. Dibble

A Thesis

Presented to the Graduate Committee

of Lehigh University

in Candidacy for the Degree of

Master of Science

in

Manufacturing Systems Engineering

Lehigh University


1986

Certificate of Approval

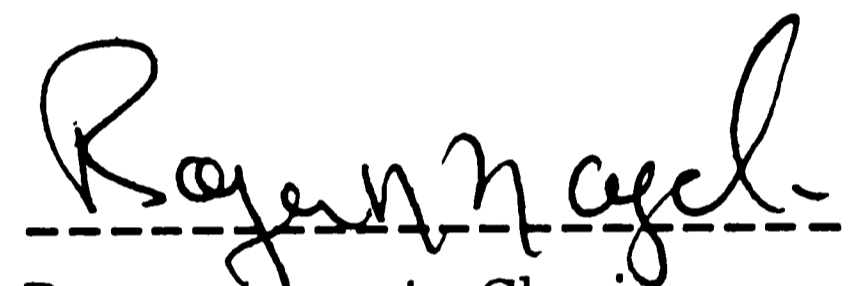
This thesis is accepted in partial fulfillment of the requirements for the degree of Master of Science

Date

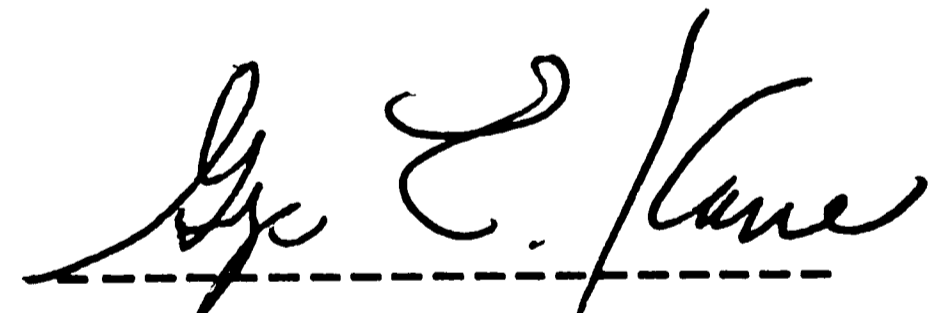
December 10, 1986

  
-----  
Professor in Charge

R.J. Jaccodine

  
-----  
Department Chairman  
Manufacturing Systems  
Engineering

Roger N. Nagel

  
-----  
Department Chairman  
Industrial Engineering

George E. Kane

## ACKNOWLEDGEMENTS

I wish to thank the following people for their help in completing this thesis;

My wife Kay for her patience and support.

My children Jessica and Melissa for fun and comic relief.

Dr. R. Jaccodine for his support and advice.

C.K. Huang for help in setting up X-Ray exposures.

Hyacinth Vedage for her advice on thesis scope.

John Barkanic for his help in running the plasma experiments.

## Table of Contents

<u>Page</u>		
	Title Page	i
	Certificate of Approval	ii
	Acknowledgements	iii
	Table of Contents	iv
	List of Figures	vi
	Abstract	1
1.0	Introduction	2
2.0	Background	
2.1	Plasma Etching - Mechanisms	5
2.1.1	Physical Etching	
2.1.2	Chemical Etching	
2.1.3	Chemical-Physical Etching	
2.2	Properties of O <sub>2</sub> /NF <sub>3</sub> and O <sub>2</sub> /CF <sub>4</sub> Discharges	9
2.3	Polyimide	12
2.3.1	Synthesis	
2.3.2	Properties	
2.4	Etching of Polyimide	15
3.0	Experimental Procedure	
3.1	Description of Apparatus	21
3.2	Sample Preparation	22
3.3	Plasma Reactor Conditions	24
3.4	Determination of Etch Rates	30
3.5	Analysis of Etch Profile	31
4.0	Results	34

5.0 Discussion	50
5.1 Step Measurements	51
5.2 Profile Shape	54
5.3 Implications	57
6.0 Summary of Conclusions	58
7.0 Recommendations for Future Research	59
References	62
Vita	64

List of Figures

<u>Number</u>	<u>Title</u>	<u>Page</u>
2.1	Illustration of Anisotropic and Isotropic Etch Profiles	17
2.2	Step 1 of Polyimide Synthesis - Polyamido Acid Formation	18
2.3	Chemical Structure of Kapton	19
2.4	Degradation Proposals for Radiated Polyimide	20
3.1	Parallel Plate Reactor Configuration	25
3.2	Sample Preparation for Experiment 1	26
3.3	Sample Preparation for Experiment 2	27
3.4	Electron Beam Exposure Set-up For Experiment 3	28
3.5	Location of Wafers on Bottom Electrode	29
3.6	Sample Step Output From Sloan Dektak	32
3.7	Sample Step Output From Taylor Hobson Talysurf	33
4.1	Measurement Positions for Experiments 1 and 2	37
4.2	Step Measurements for IR Cured (Standard) Samples	38
4.3	Step Measurements for UV Exposed Samples	39
4.4	Step Measurements for X-ray Exposed Samples	40
4.5	Step Measurements Electron Beam Exposed Samples	41
4.6	Measurement Technique from Talysurf Chart Paper	42
4.7	Comparison of Standard and Electron Beam Exposed Samples in CF <sub>4</sub> /O <sub>2</sub> Plasma	43

4.8	Comparison of Standard and Electron Beam Exposed Samples in $\text{NF}_3/\text{O}_2$ Plasma	44
4.9	Sample Set of Electron Beam vs. Standard Talysurf Traces in $\text{NF}_3/\text{O}_2$ Plasma	45
4.10	Photomicrographs of Samples NF12566 STD, NF12566 EB at 20X	46
4.11	Photomicrographs of Samples NF12566 STD, NF12566 EB at 200X	47
4.12	Talysurf Traces for PI-2566 at 5000x and 20,000x	48
4.13	Talysurf Traces for PI-2555 at 5000x and 20,000x	49

### Abstract

The effect of radiation on the etch rate of polyimide in  $\text{NF}_3/\text{O}_2$  and  $\text{CF}_4/\text{O}_2$  plasmas has been studied. Polyimide samples have been exposed to UV light, X-rays and electron beam radiation. The etch rate and profile of a step generated in the polyimide by a glass plate mask during etching have been investigated to determine the effect of the radiation.

Problems occurred in trying to reproduce step measurements, due to the variability of the measurements instruments, and the plasma reactor etch profile. A high degree of variability was observed both from sample to sample and within the same sample. A final experiment produced both a standard IR cured sample and an electron beam exposed sample on the same specimen, and a final determination of degree of etch change was made.

Radiation from the mentioned sources produced no reproducible effect on the etch rate of the polyimide. The final set of samples mentioned showed no step where the exposed/unexposed boundary was crossed. A slight effect was noticed in the film step profile with the electron beam radiation. Undercutting appeared to be less with the radiated samples, compared to the standards. SEM photomicrographs show damage was produced by the electron beam, but the damage does not produce etch rate changes.

## 1.0 INTRODUCTION

The electronics and computer industries use a large number of processes and materials to manufacture their respective products. One of the processes increasing in importance is plasma chemistry where a gas or formulation of gases is partially ionized in a vacuum to produce reactive species. A group of materials of particular interest are a group of polymers commonly known as polyimides.

Plasma processes are used extensively in the integrated circuit industry, where the process is used to define circuit patterns with a high degree of precision at micron line widths. Polyimides have been used extensively in the electronics industry in applications such as flexible circuits, encapsulants for integrated circuitry, and only recently as a substitute for silicon dioxide in integrated circuit isolation layers. This final application is where plasma processing and the characteristics of plasma treated polyimides becomes especially important. The role of plasma in this application is to open up vias for interlevel connection of circuits. The high thermal resistance and dielectric strength of polyimide make it an ideal material for isolating interlayers of circuitry, while still providing

a reasonable process to form interconnection vias.

Recent developments in polyimide chemistry have made it possible to create a photosensitive polyimide film. This is an interesting and useful development, because it makes a "permanent" photoresist possible. The polyimide could serve as a pattern mask as well as an insulating barrier for multilevel circuits, in both the ceramic and circuit board fabrication industries. In addition, polyimide is a more durable material than common photoresists, and can better withstand further processing, especially those with high temperatures.

With the invention of photodefinable polyimide, and its potential uses in defining circuit pattern, plasma chemistry and its use in defining fine line circuits will be extended to this new patterning material. The behavior of polyimide under various sources of radiation may become important in this application. The intent of this study is to determine the effect of radiation on the etch rate and profile of both normal and photo sensitive polyimides. The radiation sources used will be UV light, X-Rays, and electron beam. The effect on the etch rate and pattern of the etch will be compared using two different gas compositions. The oxygen / carbon tetrafluoride ( $O_2/CF_4$ ) system is known to produce anisotropic etch profiles in untreated polyimides, will be compared to the

oxygen / nitrogen trifluoride ( $O_2/NF_3$ ) system, which produces isotropic etch profiles.

## 2.0 BACKGROUND

### 2.1 Plasma Etching - Mechanisms

Plasma etching uses a glow discharge, usually supported by coupled radio frequency (RF) generator, to produce chemically active species from relatively inert molecular species. Once the species have been generated they can react with a surface and subsequently be pumped away by the vacuum system. Depending on the nature of the gas mixture and the substrate to be etched, there are four main plasma etching mechanisms that have been proposed [1]:

- physical etching
- chemical etching
- chemical / physical etching
- photo-chemical etching

The last of these mechanisms is not widely used in electronics manufacturing, and will not be discussed.

Three terms relating to the description of plasma treated surfaces are now defined.

Anisotropy is defined as the effect of a plasma process that creates straight sidewalls on the etched substrate. This is a desirable quality in circuit manufacture.

Isotropy is the effect of a highly reactive plasma

where the surface is undercut below the mask. Figure 2.1 illustrates anisotropy and isotropy.

Selectivity is defined by the degree of etching that takes place on all surfaces in the reactor. A process low in selectivity etches all materials at approximately the same rate.

### 2.1.1 Physical Etching

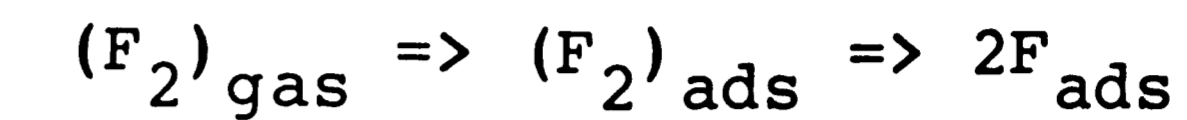
Physical etching is characterized by anisotropic etching and low selectivity. The process uses incoming ions from the plasma to sputter material off of the surface. This etching configuration normally uses an inert gas to form the plasma to give "line of sight" [1] etching of the surface. A physical bombardment of the surface is solely responsible for the etch of the substrate. In practice, however, this configuration is rarely achieved, because the ionization of the incoming gases in the plasma usually generate species that are both energetic and chemically reactive.

### 2.1.2 Chemical Etching

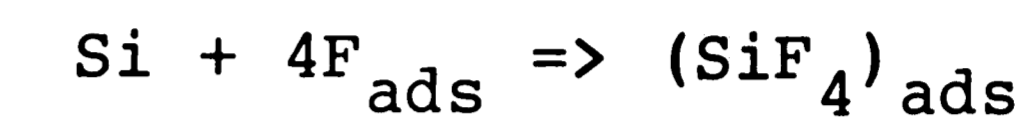
Chemical etching in a plasma is characterized by an isotropic, selective etch profile. The plasma's only role in a pure chemical etching environment is to produce the reactive chemical species through molecular collisions in the feed gas. Coburn and Winters have proposed a

mechanism for the surface etching process using the silicon/fluorine reaction as an illustration [2]:

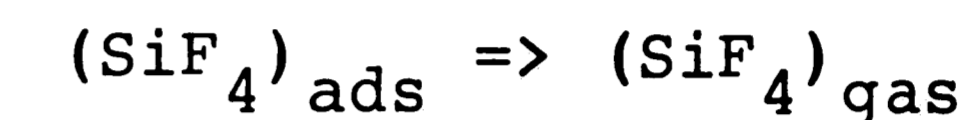
1. Chemisorption:



2. Reaction:



3. Desorption:



In the chemical etching system, different combinations of reactant gases and surfaces will determine the rate limiting step of the reaction. For example,  $\text{CF}_4$ ,  $\text{CF}_3\text{H}$ ,  $\text{CF}_3\text{Cl}$ ,  $\text{CF}_2\text{Cl}_2$ , and  $\text{CCl}_4$  do not spontaneously chemisorb on silicon, thus revealing step 1 as the rate limiting step [3]. On the other hand, chlorine does chemisorb on silicon, but is stable at room temperature. This suggests that step 2, the formation of a reactant product is the rate limiting step [4,5].

In summary then, chemical etching is selective due to the reactivity of different surfaces to the chemical properties of the plasma, is isotropic since the ionized particles provided by the plasma plays no "line of sight" role in etching the substrate, and is controlled by the three mechanisms mentioned above, chemisorption, reaction, and desorption.



### 2.1.3 Chemical - Physical Etching

As mentioned in the characterization of physical etching, a pure chemical or physical plasma reaction environment rarely exists. The most difficult of the three primary mechanisms to understand is ion assisted plasma chemistry, or what is sometimes called chemical-physical plasma etching. The difficulty arises due to the variability in the chemical or physical properties of the etchant gas combinations. Three mechanisms for this process that have been suggested.

Chuang, Tu, and Winters proposed that ions may sputter away absorbed reaction products on the substrate, thereby increasing the rate of the desorption step. At the same time, this increases the availability of reaction sites, further increasing the substrate etch [6].

Mogab and Levenstein propose that the impinging ions produce damage in the lattice structure of the surface, creating chemically "vulnerable" sites. These sites are subject to reactions that can proceed at an accelerated rate [7]. The explanation offered by these authors is contrary to Winters and his coworkers. This illustrates the complexity of the process at hand.

The third mechanism, by Bruce, tries to explain the presence of anisotropic etching in chemical-physical systems. Some gases that are used in processes or are

intentionally introduced into other processes can break down into unsaturated radicals and ions that adsorb to etched sidewalls. Since these areas are not subject to vigorous line of sight bombardment from the ion on the plasma, these compounds can become quite thick, or are quite tenacious, thus prohibiting a chemical etching effect in the horizontal direction [8].

The actual mechanism observed in physical-chemical etching is probably a combination of all of these proposed mechanisms.

The large number of combinations of etching gases, reactor conditions, and surfaces further complicate the etching process. Due to these complexities, chemical-physical etching parameters used in practice are necessarily found through experimentation.

### 2.2 Properties of $CF_4/O_2$ and $NF_3/O_2$ Discharges

The etch gases of interest in this study are  $CF_4/O_2$  and  $NF_3/O_2$  combinations.  $CF_4$  has been widely used as an etchant for silicon, and its combination with a small amount (10 - 30%) of oxygen increases the silicon etch rate by as much as 3.5 times [2]. Harsburger and coworkers first published results noting that when oxygen was introduced into a  $CF_4$  discharge, there was a correlation between the fluorine and carbon monoxide

optical emission, and the etch rate of silicon [9]. Their conclusion is that an increase in active fluorine atom density is responsible for the higher silicon etch rate.

Coburn and Winters suggest three reasons why the oxygen addition has such a dramatic positive effect [2]. First, gas phase fluorocarbon radicals can oxidize, leading to the more difficult production of fluorine atoms. Second, the carbon that resides on the walls of the reactor system can oxidize, serving to decrease recombination reactions that consume fluorine, making it unavailable for etching. Third, fluorocarbons that are deposited directly on the reactor surfaces oxidize and create fluorine directly.

An analogous situation to the silicon example occurs when polymers are being etched in an oxygen discharge, and small amounts of  $CF_4$ ,  $NF_3$ , or  $SF_6$  are added to the discharge. Egitto et. al. concluded that the enhancement in etch rate is due to the inclusion of fluorine in the polymer structure, making reaction sites available. However, when an excess of fluorine exists, passivation of the surface reaction sites can occur, inhibiting the reaction rate [10]. This phenomena has also been noted by others [11,12,13]. O'Grady's work with the  $O_2/NF_3$  system shows a desirable increase in the polymer etch rate compared to the  $O_2/CF_4$  system.

$NF_3$  is gaining attention as both a silicon and polymer etchant gas. The interest in  $NF_3$  stems from unique properties of the gas compared to other etchants.

The  $NF_3$  molecule dissociates more readily than  $CF_4$  [14]. The following reaction step comparisons illustrate this property:

<u>Reaction</u>	<u>Dissociation Energy</u> (kcal/mol)
$NF_3 \Rightarrow NF_2 + F$	59
$NF_2 \Rightarrow NF + F$	58
$CF_4 \Rightarrow CF_3 + F$	130
$CF_3 \Rightarrow CF_2 + F$	87

A process that uses  $NF_3$  instead of two other possibilities,  $CF_4$  or  $SF_6$ , does not leave behind a polymeric or carbonaceous residue. A lower carbon partial pressure is exhibited because there is no carbon in the feed gas. This serves to make fluorine atoms available for etching, instead of competing with feed gas carbon or sulfur atoms. Another side benefit of both  $NF_3$  and  $SF_6$  are that the carbon atoms present in the off gas can be analyzed using a mass spectroscopic technique to understand the plasma process. Since the feed gases contain no carbon, the carbon containing off gasses are direct reaction products or system contaminants.

The high reactivity of  $\text{NF}_3$  can be tailored with the introduction of small percentages of fluorinated halocarbons [15], that aid in the production of a sidewall passivation as suggested by Bruce. This recent development highlights the usefulness of  $\text{NF}_3$ , and shows a tailoring process applied.

Both the  $\text{O}_2/\text{CF}_4$  and  $\text{O}_2/\text{NF}_3$  systems are examples of chemical-physical etching systems. Due to the dissociation energy differences, and the high reactivity of the  $\text{NF}_3$  combination, a more isotropic etch profile can be expected with the  $\text{NF}_3$  system.

## 2.3 Polyimide

### 2.3.1 Synthesis

Polyimide can be made through many different reaction combinations, but the most popular method was a two step process developed at DuPont in 1959 [16].

The first process step uses a combination of dianhydrides of tetracarboxylic acids in a reaction with aromatic diamines in the presence of a suitable solvent such as dimethyl sulfoxide or N-methyl 2 pyrrolidone to form a polyamido acid. Depending on the radical groups attached to the reactants, different polyamido acids can be formed. A sample reaction mechanism is illustrated in Figure 2.2.

The second step, known as imidization, is a dehydration step that can be performed in two ways, thermal or chemical. The thermal step involves heating the polyamido acid in vacuum or in an inert atmosphere above  $200^\circ\text{C}$  to drive off the water. Chemical cures use dehydrating agents such as acetic anhydride to extract the water.

The chemical form of a popular polyimide known as Kapton<sup>1</sup> is shown in Figure 2.3.

### 2.3.2 Properties

After curing, polyimide becomes a faintly yellow transparent film, typically with excellent tensile strength and elasticity. A tensile strength of  $1200\text{ kg/cm}^2$ , and an elongation of 80% at fracture are common. Further, polyimides do not "melt" as some other aromatic or chain polymers do. Rather the literature refers to a "softening point" where the material begins to oxidize, and therefore degrades. Softening point temperature ranges are between  $400^\circ - 600^\circ\text{C}$ .

In chemical environments, polyimide is stable in organic solvents such as alcohols, and is not significantly affected by mild acid environments. However, the material will degrade in strong acids such as

---

<sup>1</sup> Kapton is a trademark of E.I. du Pont de Nemours & Co.

fuming nitric and hot concentrated sulfuric acids. Polyimides behave poorly in alkaline environments and under exposure to superheated steam. The susceptibility is due mainly to breaking of the C=O groups [17]. See the structure in Figure 2.3.

Polyimide is also a material of interest in the aerospace industry. Because of its high temperature resistance, polyimide has been employed to withstand the thermal shock of satellite launching. After the satellite is in service the polyimide coatings are subject to considerable thermal, vacuum and radiation exposures. A study by Chaturvedi et. al [18] found that polyimides degrade somewhat under bombardment by protons and neutral ionic species. The proposed mechanism is either an opening in the imide ring, or the scission of the polymer to create a series of monomer reaction sites. An illustration of these proposals is found in Figure 2.4.

The electrical properties of polyimide are especially important in the application of the material in computers and electronics. A study by Rothman [19] showed that the dielectric strength of polyimide was not as good as sputtered SiO<sub>2</sub>. An average value of  $6.25 \times 10^6$  V/cm for seven polyimide samples was found compared to a value of  $8.60 \times 10^6$  V/cm for sputtered SiO<sub>2</sub>. However, this difference is not large enough to preclude the use of

polyimide as a substitute for silicon dioxide in some appropriate integrated circuit applications.

#### 2.4 Etching of Polyimide

Studies of etching polyimide have been reported in the literature, mainly with the O<sub>2</sub>/CF<sub>4</sub> system.

Turban and Rapeaux [11] found that the etch rates with the O<sub>2</sub>/CF<sub>4</sub> system are high, on the order of .5 - 3 um/min. There is no evidence of a loading effect at low pressures (.2 torr), but such an effect is present at higher pressure. The optimum CF<sub>4</sub> concentration was 20% of the total feed. The effect of temperature was noted in this study; an increase in the reactor chamber temperature results in a higher etch rate through increased reaction kinetics.

Egitto et. al. [10] found similar results, but at a CF<sub>4</sub> concentration of 22.7 %. The highest rate found in this study was 1.5 um/min. A higher amount of CF<sub>4</sub> in the feed gas contributes to the formation of CF<sub>2</sub> on the polyimide, thus lowering the etch rate. Therefore, these contributors theorize that a specific level percentage of F/O atoms exists that produces the maximum etch rate. A higher fraction than optimum will result in lower etch rates due to passivation layers growing on the substrate. A lower fraction than optimum results in a lower etch rate

due to a lack of reactive fluorine atoms.

Purushothaman et. al. [12] found an optimum  $\text{CF}_4$  concentration at 27% of the feed gas. In addition these workers found the same correlation between substrate temperature and etch rate as Turban and Rapeaux.

A master's thesis has been done at Lehigh University using  $\text{NF}_3/\text{O}_2$  to etch a polymer. O'Grady's work [13] showed a significant etch rate advantage for the  $\text{NF}_3/\text{O}_2$  combination at low power compared to  $\text{CF}_4/\text{O}_2$  for Shipley AZ 1350 J photoresist. Figure IV illustrates the trend of etch rate vs. power at a 10 %  $\text{NF}_3$  or  $\text{CF}_4$  combination in  $\text{O}_2$ . Perhaps a more striking advantage is illustrated in Figure V. At low power, the etch rate of the  $\text{NF}_3/\text{O}_2$  combination is approximately three times the rate of the  $\text{CF}_4/\text{O}_2$ . The work was extended to polyimide, but etch rates were not studied. However, the profile of the  $\text{NF}_3/\text{O}_2$  etch was determined to be anisotropic, as predicted.

The parameters for this study will be an extension of O'Grady's work, using an average power value of 500 watts aimed at the determination in etch rate differences, and wall profile differences in the two gas combinations as well as other factors.

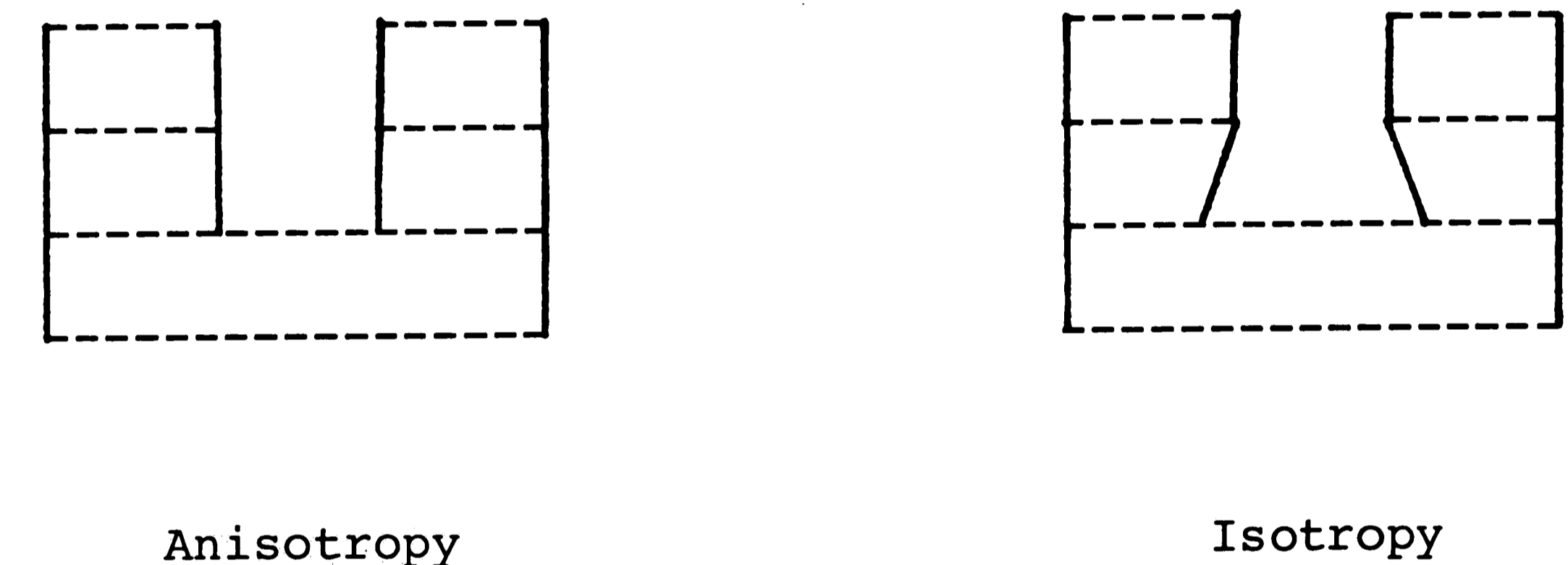


Figure 2.1 Illustration of Anisotropic and Isotropic Etch Profiles

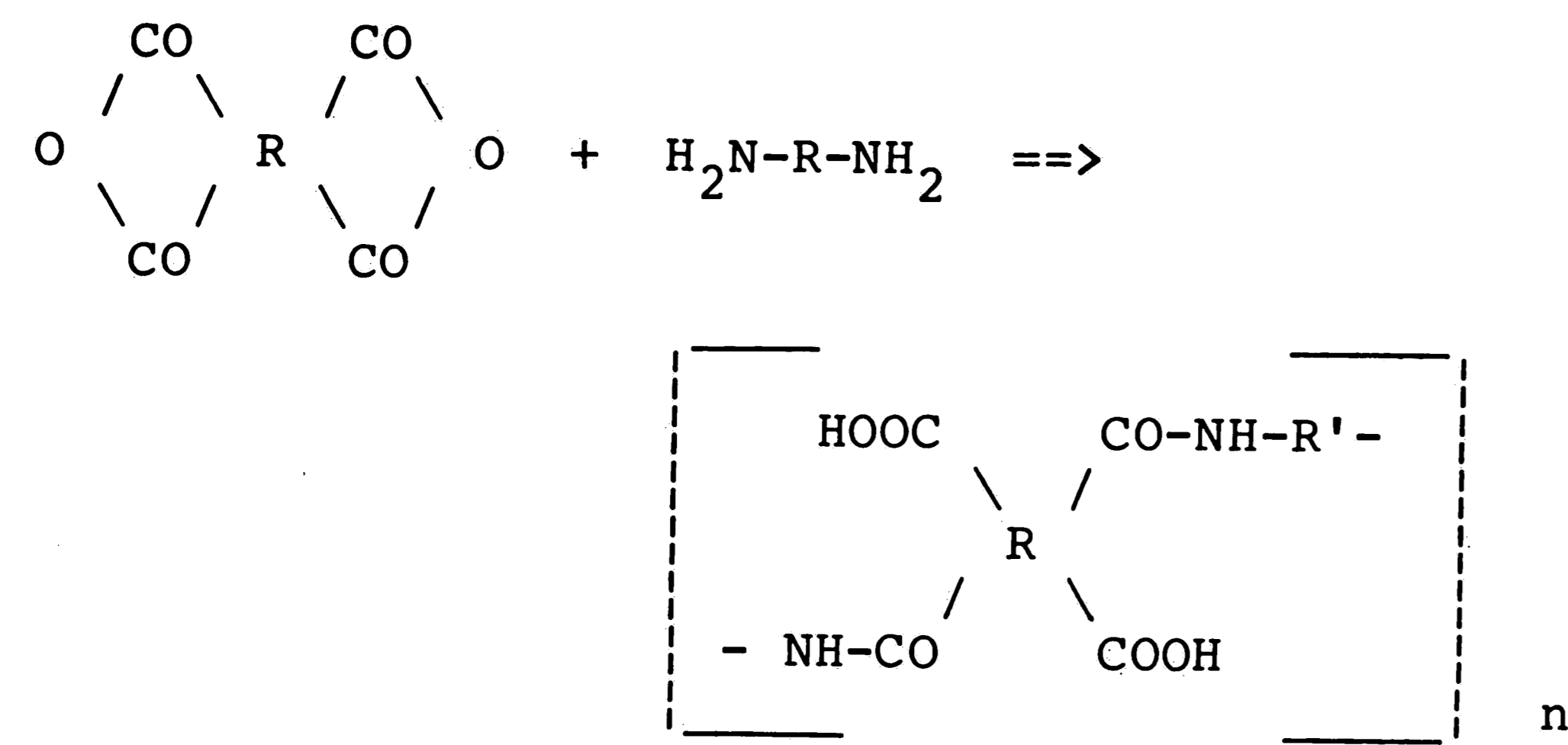


Figure 2.2 Step 1 of Polyimide Synthesis - Polyamido Acid Formation

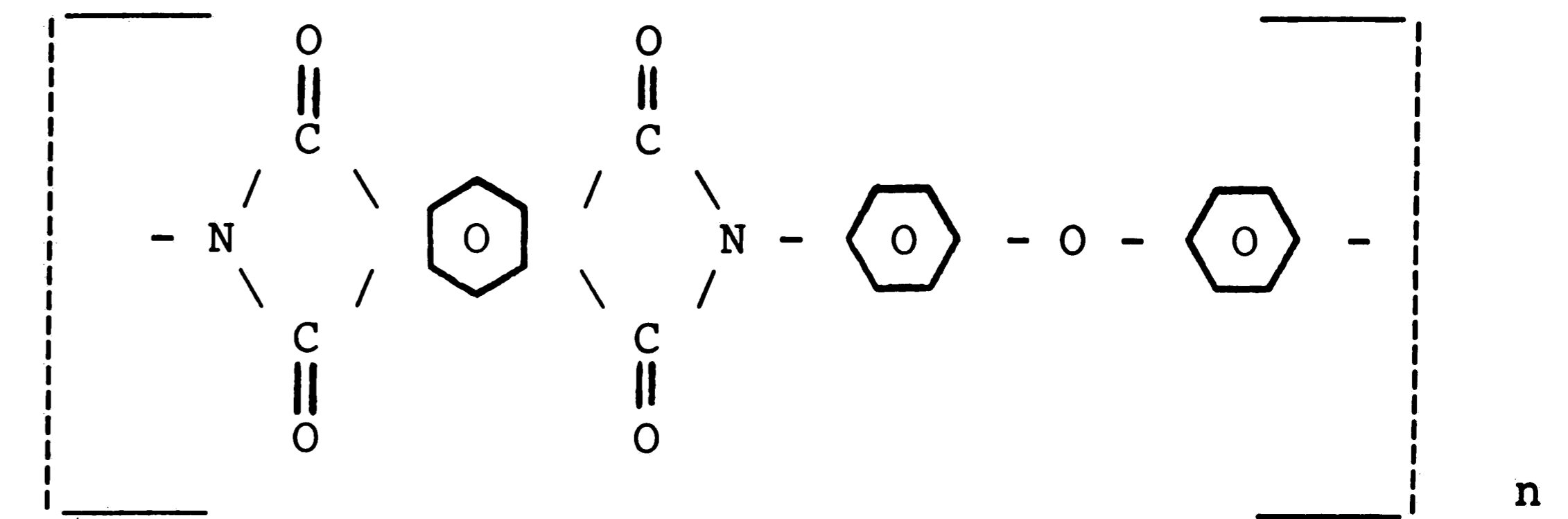


Figure 2.3 Chemical Structure of Kapton

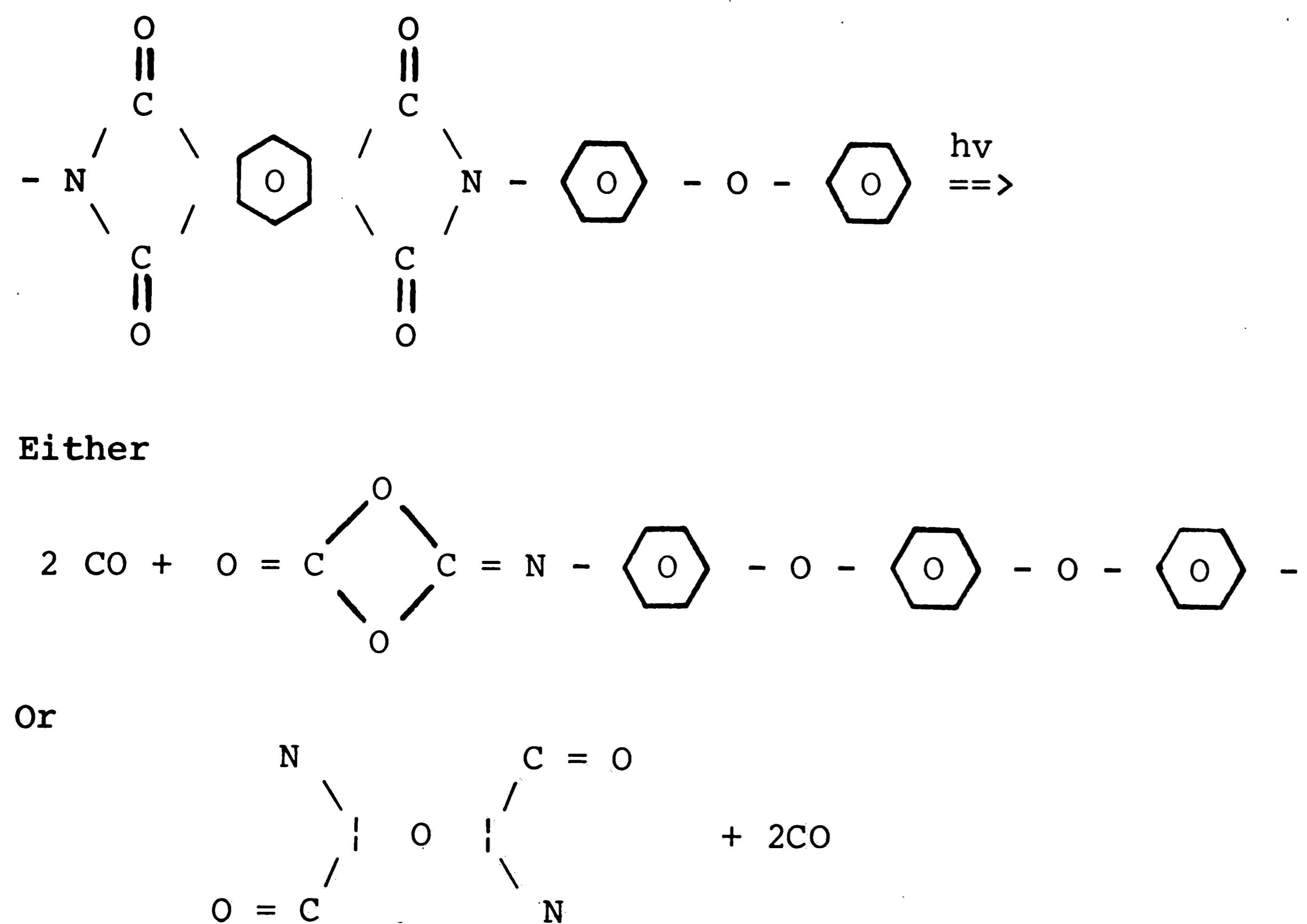


Figure 2.4 Degradation Proposals for Radiated Polyimide

### 3.0 Experimental Procedure

#### 3.1 Description of Apparatus

All of the etching in this study was done on a Plasma-Therm PK2440 parallel plate reactor, as illustrated in Figure 3.1. The aluminum parallel plates were 53.3 centimeters in diameter at a spacing of 3 cm. The electrodes were powered at a radio frequency (rf) of 13.56 MHz. Mass flow controllers were employed to provide consistent gas flow to the reactor chamber. The chamber was maintained under vacuum by an Alcatel model ZT 2063C two stage mechanical pump. A Neslab HX-150 Refrigerated Recirculating Heat Exchanger was used to maintain the temperature of the electrodes in the reaction chamber at 17° C.

Samples were exposed to radiation from three different sources, UV, X-Ray, and Electron beam.

UV exposures were done in 15, 30 and 45 second doses of UV light from a mercury source on a Cobilt exposure tool.

X-Ray exposures were done with a Rigaku Denki Co. Ltd. "Rota Unit" High Power Constant Potential Rotating Anode Microfocus X-Ray generator. The samples were mounted to a Krystallos motor driven XY stage. The sample passed in front of the 1 millimeter slit from the x-ray

generator. Increasing exposure was accomplished by multiple passes.

Electron beam exposures were done with a High Voltage Engineering Corporation Van de Graff Generator Model Kn-2. A stand and fixture was arranged 40 centimeters from the beam opening to spread the beam to the full diameter of the sample.

### 3.2 Sample Preparation

The first set of samples were 8.25 centimeter (3 1/4 inch) silicon wafers coated with DuPont 5878 polyimide, cured at 360°C. The average thickness of polyimide on the samples was 10 microns. A series of radiation exposures was done to provide a benchmark for a comparison experiment on new Dupont polyimides. The matrix of samples prepared is illustrated in Figure 3.2.

The exposures on the UV tool were from a mercury lamp source. The exposure time was maintained with a stopwatch.

The total exposure time given for the x-ray exposures were calculated based on a stage speed of .63 cm/min, and a an x-ray exposure width after some spreading, of 2 mm. An exact calibration of the stage movement was not possible for the precision desired, so the values listed are higher than the desired 15 second intervals found in the UV exposure. The x-ray was emitted from a rotating

silver source, originating from a 35 kV, 5 mA electron beam.

Exposure times on the Van de Graff generator were controlled by an electric timer. The measured absorbed electron beam current was 10 uA, at a voltage of 2 Million Electron Volts (MeV).

The second set of samples consisted of DuPont PI-2566, PI-2555, and PI-2525 polyimides coated on 10.16 cm (4 inch) silicon wafers. The PI samples were supplied precoated by DuPont, so the thickness of the coating was unknown. The samples listed in Figure 3.3 were exposed to electron beam radiation for 45 second at 2 MeV, and an absorbed beam current of 10 uA.

Each silicon wafer was cleaved into quarters and the polyimide coating carefully cut with a razor blade, leaving it intact for etching.

The third set of samples were drawn, one each, from the DuPont PI sample polyimides. Each of the wafers was exposed to the electron beam for 45 seconds at the same beam parameters listed in Figures 3.2 and 3.3, with half the wafer shielded by a semicircle of lead, approximately 60 mm thick.

The purpose of this final experiment was to provide a standard and exposed sample on the same wafer, making detection of an etch rate effect easier to measure. A



schematic of the exposure set-up is shown in Figure 3.4.

### 3.3 Plasma Reactor Conditions

All of the etching experiments were performed at the parameters given:

- Gas Flow Total - 50 sccm
- Power - 500 W
- Pressure - 500 mTorr
- Gas Compositions - 25%  $\text{NF}_3$  in  $\text{O}_2$  or 30%  $\text{CF}_4$  in  $\text{O}_2$

The location of the wafer quarters in the plasma reaction chamber for experiments 1 and 2 are shown in Figure 3.5. In the figure location "B" is also noted as the location for the 100 centimeter wafer used in the third experiment. The samples in experiments 1 and 2 were shielded to obtain an etched step by placing a glass slide over one half the wafer.

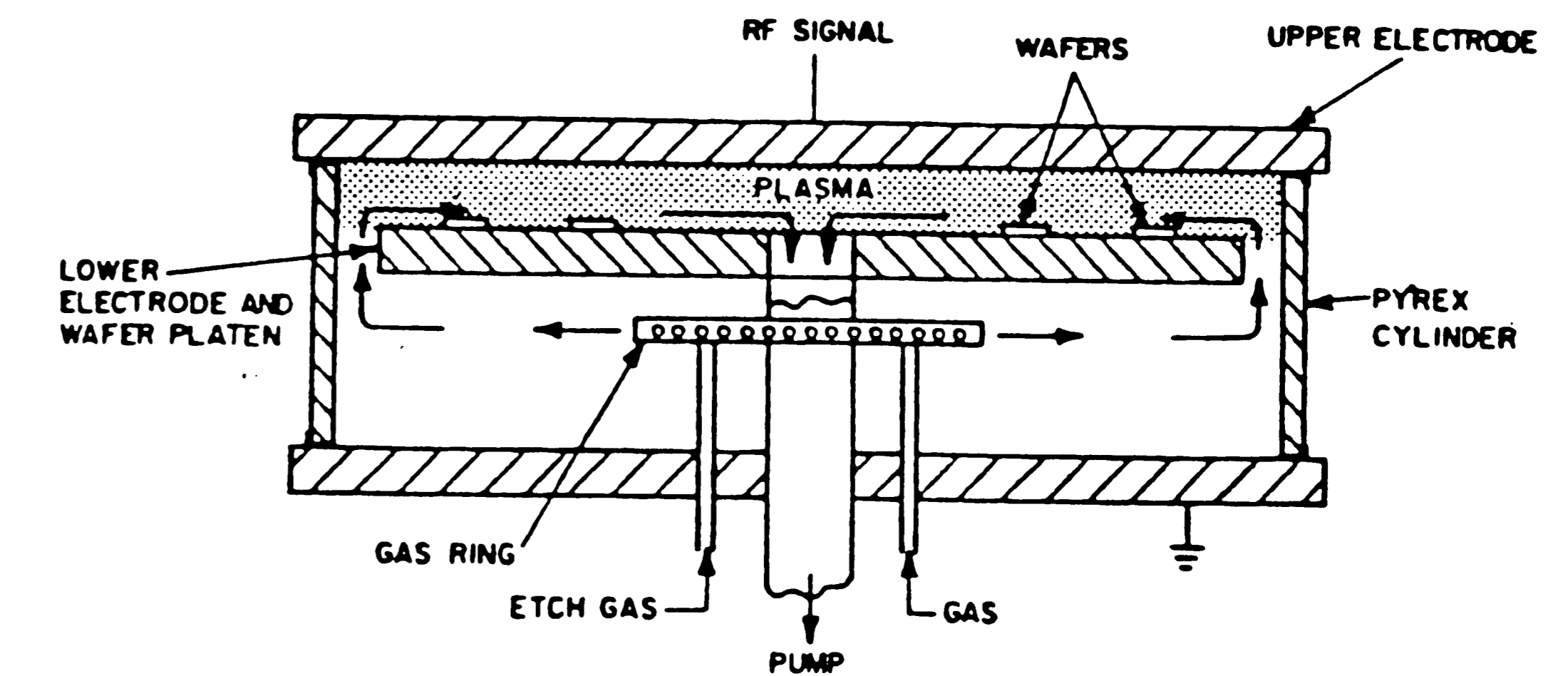


Figure 3.1. Parallel plate reactor configuration.

Radiation Source	Exposure Time (sec)	Code Prefix
Infrared	--	IR
Ultraviolet	15	UV1
	30	UV2
	45	UV3
X-Ray	19	XR1
	38	XR2
	57	XR3
Electron Beam	30	EB1
	45	EB2

Coding Example: UV1NFB - Exposure UV1, Etched in  $NF_3/O_2$ , Position B

Figure 3.2. Sample preparation for experiment 1.

Radiation Source	Exposure Time (sec)	Code Prefix
Infrared	--	STD
Electron Beam	45	EB

Coding Example: NFA2545EB -  $NF_3/O_2$  Etch, Position A, Polyimide 2545, Electron Beam Exposure

Figure 3.3. Sample preparation for experiment 2.

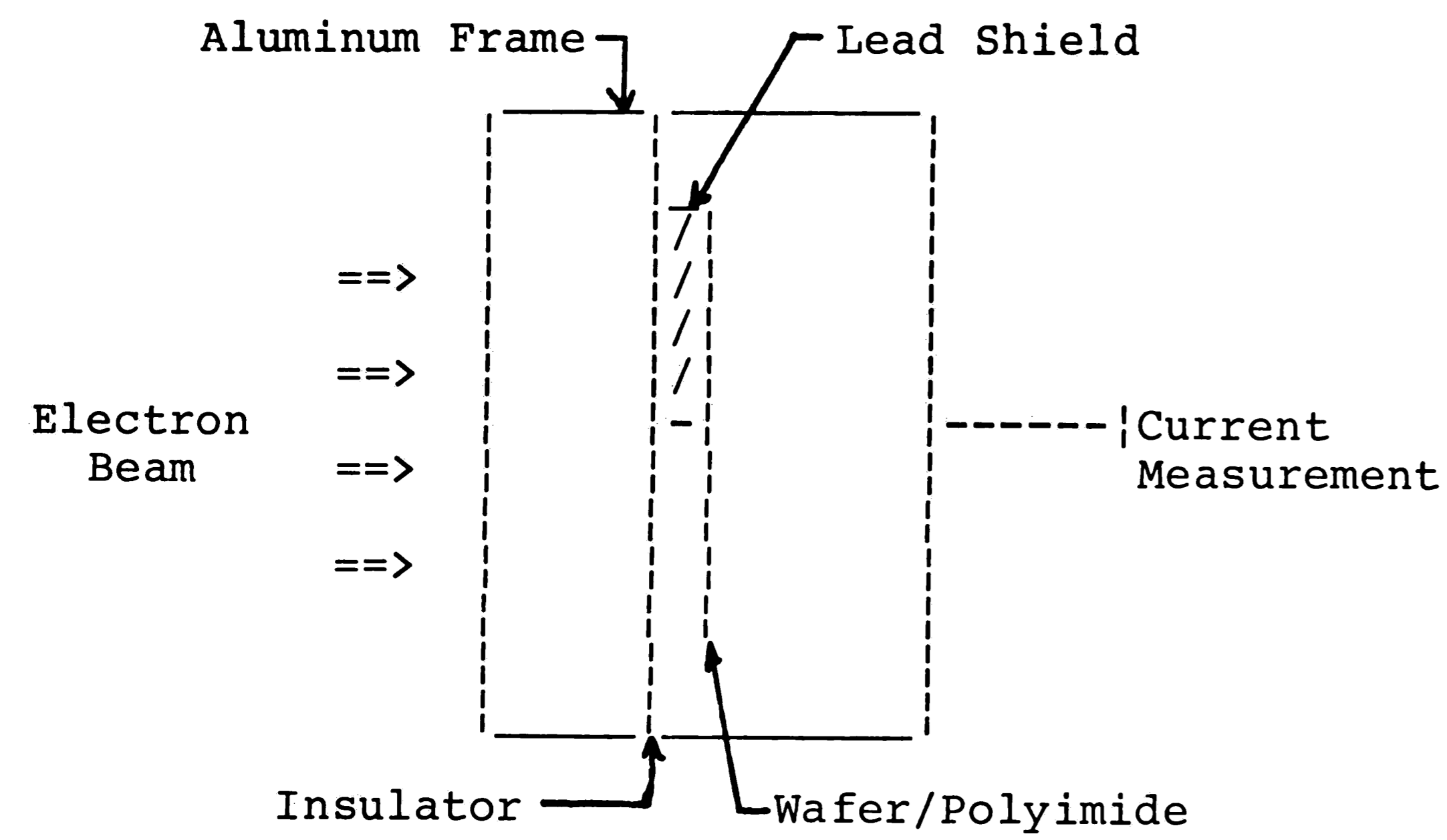


Figure 3.4. Electron Beam Exposure Set-up for Experiment 3

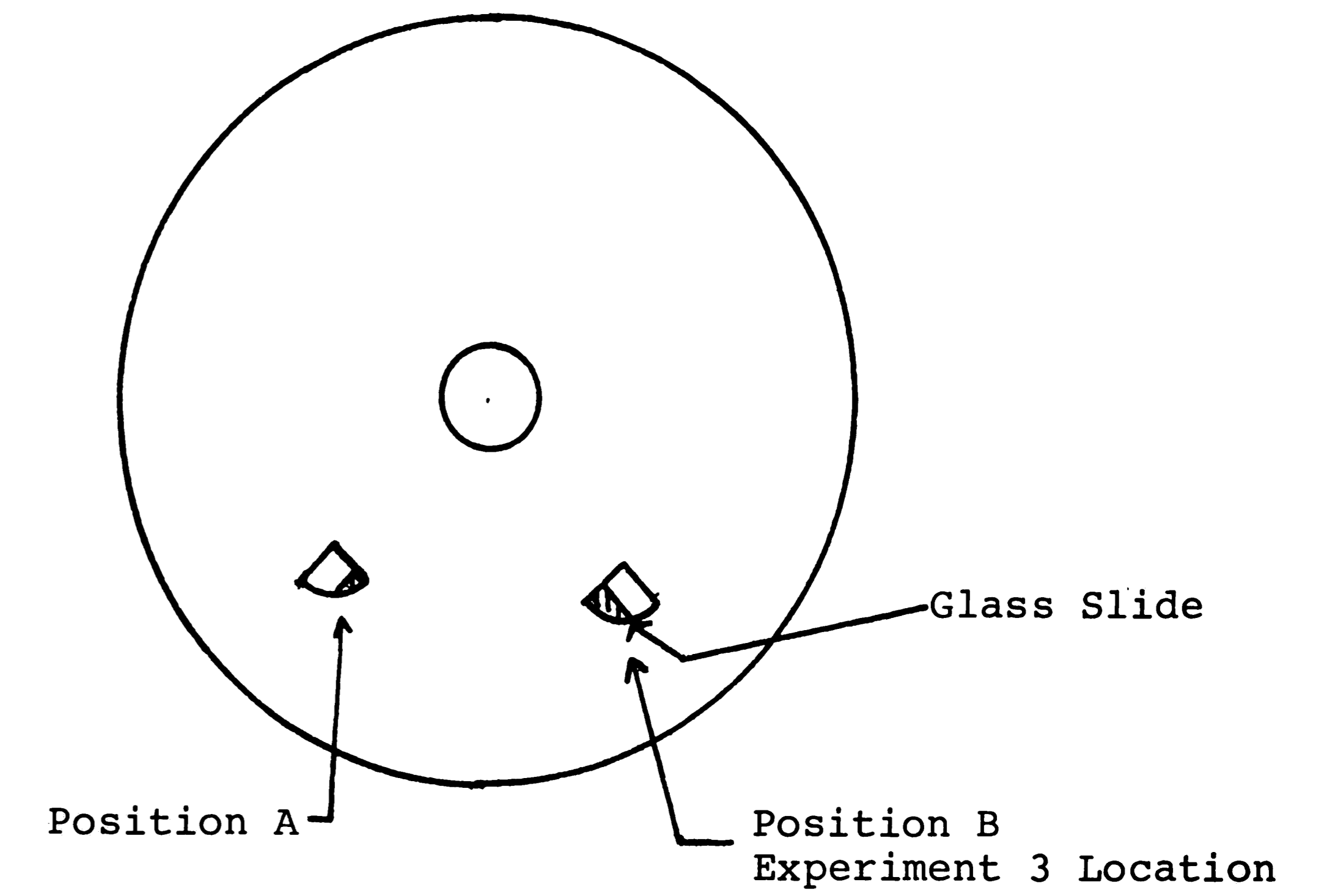


Figure 3.5. Location of Wafer Sections on Bottom Electrode

### 3.4 Determination of Etch Rates

The etch rates for the plasma treated polyimide were determined by a step measurement method. During the etching of each sample in the plasma chamber, a laboratory glass sample slide was put on top of half the silicon wafer quarter to isolate the polyimide underneath from the physical effects of the plasma.

Samples from the first experiment were measured for step height on a Sloan Dektak Model II. A sample of the output from the instrument is given in Figure 3.6. Aside from the set-up information such as scan speed and ID information, the location and difference in positions of the trace at cursors R and M are especially important. The upper right corner of the figure shows a calculated difference in trace height of at the two cursor location, shown overlaying the trace. The step height of this value in angstrom units.

The second and third set of step height measurements were done on a Taylor Hobson Talysurf Model 5-120. A typical "talysurf" trace is illustrated in Figure 3.7. The talysurf trace is harder to read, because the pickup needle is more sensitive, and an automatic leveling feature is not included as it is on the Dektak.

### 3.5 Analysis of Etch Profile

The direction of the etch, and the determination of anisotropy were attempted through examination on an ETEC Corporation Autoscan scanning electron microscope (SEM). Photomicrographs were taken to illustrate the difference in etch topography between the side shielded with the glass plate, and the difference in topography between electron beam exposed polyimide and standard, IR cured polyimide. Due to the nonconductive nature of the specimens, they were sputtered with 80% gold 20% palladium in a Poaron E5100 Sputter Coater prior to evaluation.

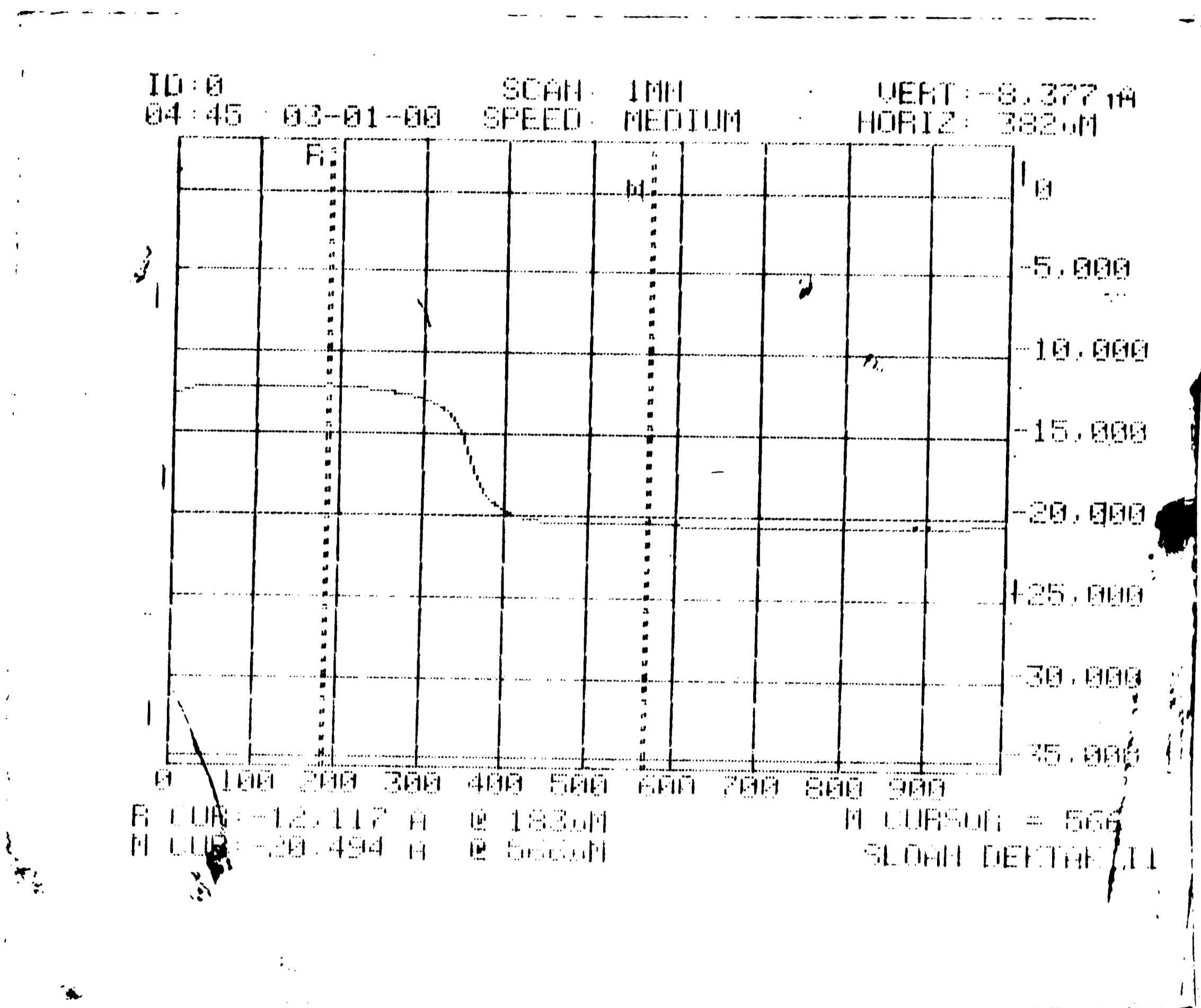


Figure 3.6. Sample output from Sloan Dektak

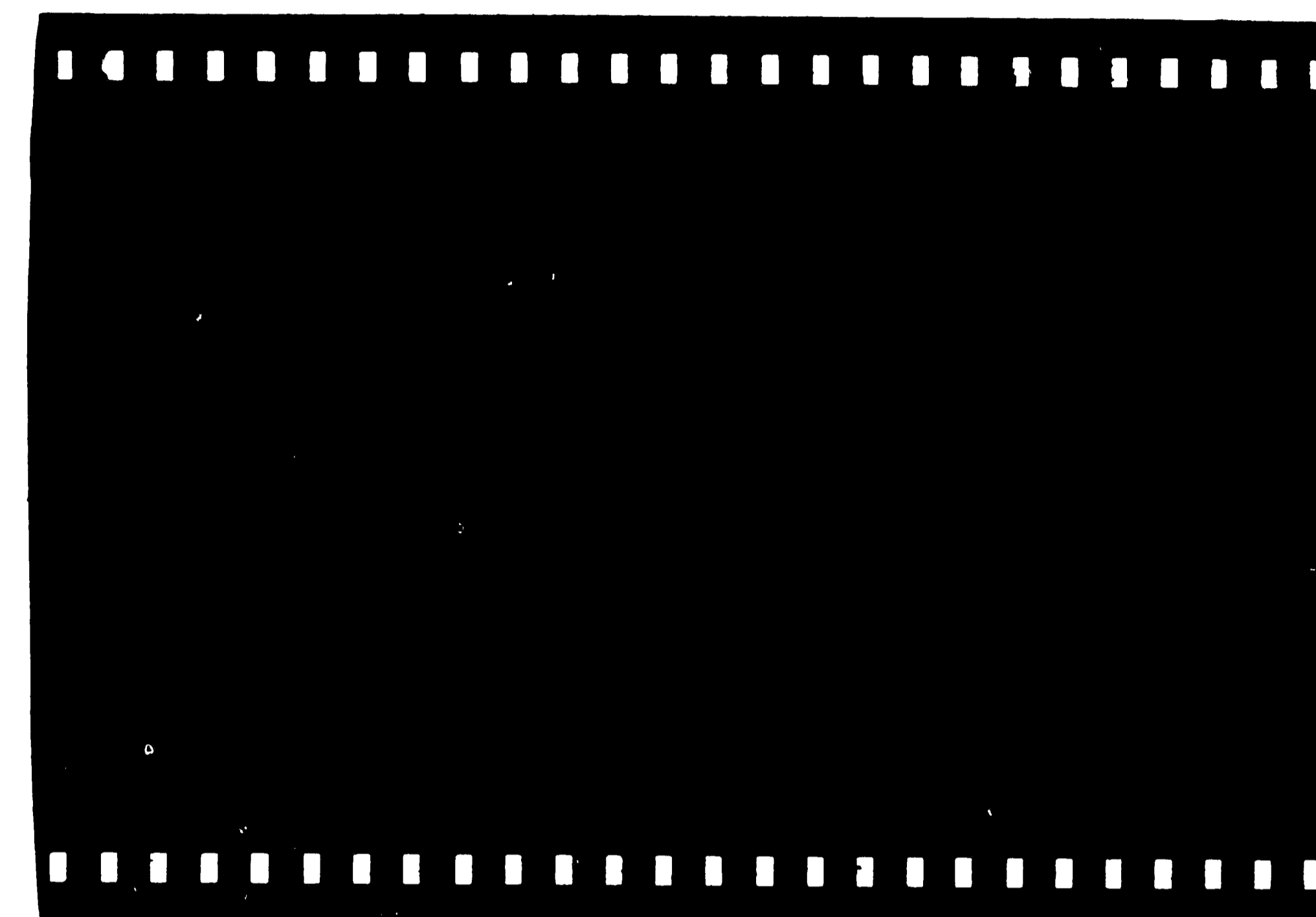
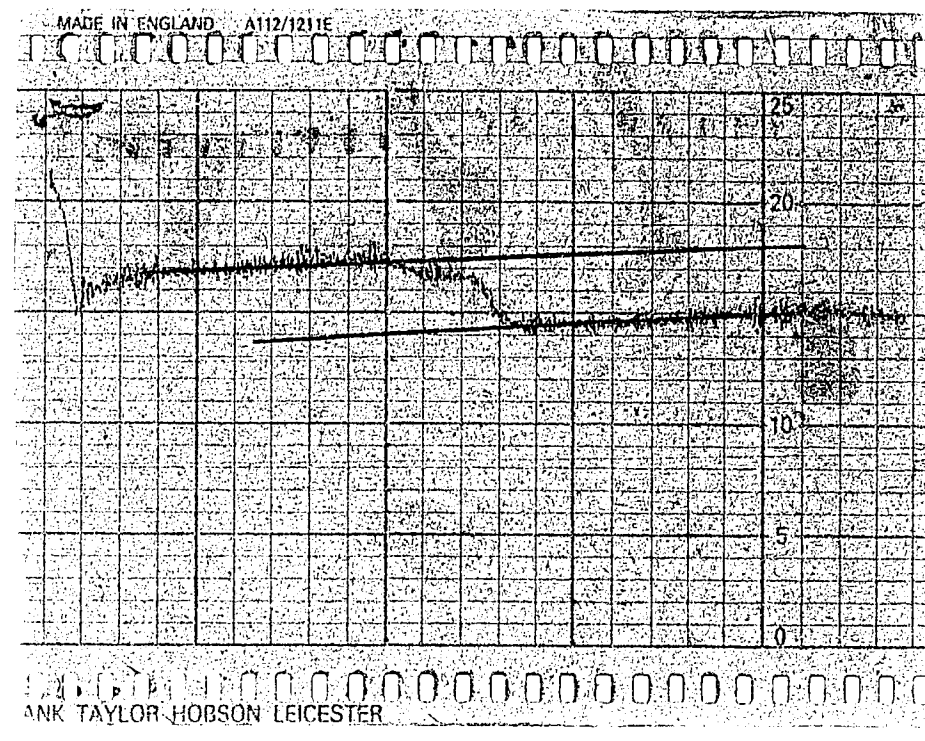


Figure 3.7. Sample output from Taylor Hobson Talysurf



#### 4.0 Results

The profiles created by the Dektak and Talysurf were taken from three spots on the sample. Positions 1 and 3 were selected at random near each edge, and position 2 was selected approximately at the center of the sample. Figure 4.1 illustrates the approximate measurement positions for experiments 1 and 2, where quartered silicon wafers were used.

The results of the first experiment, where samples of DuPont 5878 polyimide were exposed to various forms of radiation, are grouped in Figures 4.2 - 4.5. Each table is labeled for positions 1 - 3 across the top of the table. The average of two measurements (when possible) by Dektak is given next to the sample code previously described in Figure 3.2.

The second group of samples were more difficult to read, since the Talysurf does not read the step automatically. To calculate the step height, the talysurf trace was aligned with a straight edge prior to and after the step, so that a difference in the etch rates could be calculated. Figure 4.6 shows this procedure, with the divisions in the chart paper representing 5 microinches, or approximately .125 micron.

Figure 4.7 supplies the averages of two readings at positions 1 - 3 for a comparison of standard, IR cured

sample vs. the electron beam exposed polyimide in  $CF_4/O_2$  plasma. The same data is reproduced for the  $NF_3/O_2$  system in Figure 4.8.

A slight difference was noted in the etching of the polyimides in the  $NF_3/O_2$  system when the shape of the curves from the talysurf for the electron beam exposed and standard polyimide were compared. A sample set of traces are given in Figure 4.9.

To verify the step profile difference, an attempt was made to use the SEM to make photomicrographs. The results are not indicative of a difference in the step profile, but rather indicate a difference in the morphology of the exposed and unexposed polyimide. Photomicrographs of two samples, NF12566 STD and NF12566 EB are compared at 20X in Figure 4.10, and at 200X in Figure 4.11.

The results of the shielding experiment are given in Figures 4.12 and 4.13. The third polyimide PI 2545, was totally etched away, and therefore provided no data for a third figure. The top talysurf trace is labeled 5000x, and was used to find the curvature of the sample. The two example traces below are typical examples of traces on that sample at a 20,000x magnification. A vertical division on the 5000x chart represents .5 micron, whereas the same division on the 20,000x chart represents .125 micron. On each of the charts a cross hatch is made.

This represents the point at which the talysurf needle passed over the Electron beam exposed/unexposed border.

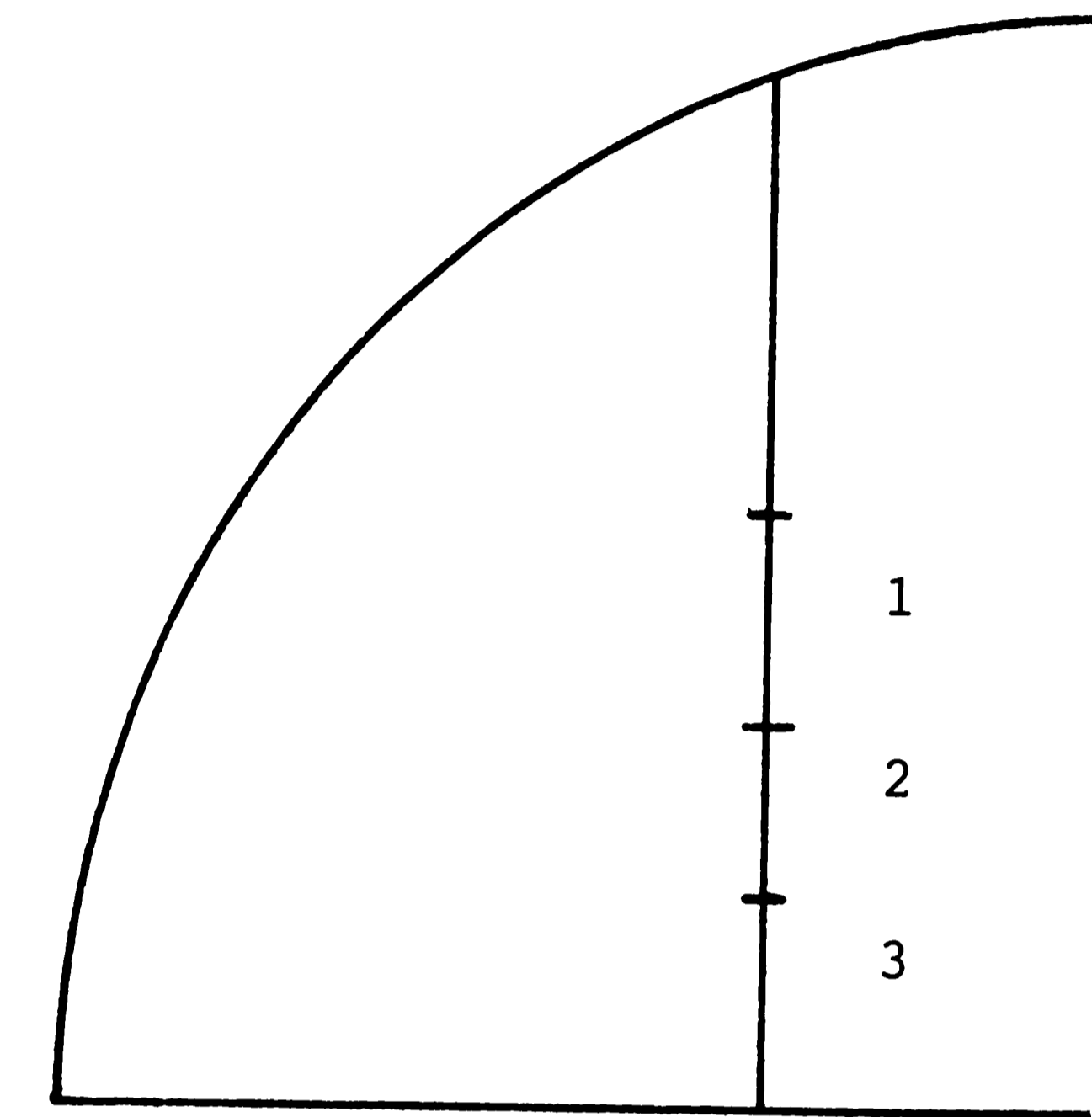


Figure 4.1. Measurement Positions for Experiments 1 and 2



Step Measurement (Angstroms)

Sample Code	Position		
	1	2	3
IRNFA	Not visible in microscope		
IRNFB	3297	3721	3409
IRCFA	6605	6437	4749
IRCFB	2238	3144	3752

Figure 4.2. Step Measurements for IR Samples - Experiment 1

Step Measurement (Angstroms)

Chamber Loc	Expose Time (sec)	Position		
		1	2	3
		***NF <sub>3</sub> /O <sub>2</sub> ***		
	15	7917	8399	5154
A	30	4994	4574	3873
	45	Not visible in microscope		
---	15	6466	5282	6264
B	30	4962	3785	2455
	45	4329	4848	3479
		***CF <sub>4</sub> /O <sub>2</sub> ***		
	15	2613	3328	2459
A	30	3688	1707	2153
	45	3552	3722	4124
---	15	2805	2256	3399
B	30	3809	4347	4898
	45	2325	3635	4013

Figure 4.3. Step Measurements for UV Samples - Experiment 1

Step Measurement (Angstroms)

Chamber Loc	Expose Time (sec)	Position		
		1	2	3
		***NF <sub>3</sub> /O <sub>2</sub> ***		
	19	7314	6407	4789
A	38	5067	4872	3857
	57	5428	5912	5561
---	19	Not visible in microscope		
B	38	2246	2813	--
	57	3921	3301	2972
		***CF <sub>4</sub> /O <sub>2</sub> ***		
	19	2401	2246	1608
A	38	Not visible in microscope		
	57	2762	2746	2543
---	19	2923	3058	2653
B	38	2752	2952	2686
	57	Sample broken in transit		

Figure 4.4. Step Measurements for X-Ray Samples - Experiment 1

Step Measurement (Angstroms)

Chamber Loc	Expose Time (sec)	Position		
		1	2	3
		***NF <sub>3</sub> /O <sub>2</sub> ***		
	15	3114	4118	2485
A	30	Not visible in microscope		
---	15	Not visible in microscope		
B	30	3225	3723	1583
		***CF <sub>4</sub> /O <sub>2</sub> ***		
	15	3459	2306	1918
A	30	Not visible in microscope		
---	15	Not visible in microscope		
B	30	1713	--	--

Figure 4.5. Step Measurements for Electron Beam Samples - Experiment 1

Measurement Reference Lines



Figure 4.6. Measurement Technique from Talysurf Chart Paper

Step Measurement (Angstroms)

Sample Code	<u>Standard IR Cure</u>			<u>Electron Beam</u>		
	Position 1	Position 2	Position 3	Position 1	Position 2	Position 3
A2545	2750	2600	2700	2850	1810	1250
B2545	3700	2700	2500	3850	4700	3750
A2555	3350	4870	2000	2500	1850	2000
B2555	4600	4600	4750	3350	3370	3120
A2566	4500	4850	5250	3350	4100	5100
B2566	4950	4200	4750	3100	3350	3620

Coding Example: A2545 - Position A in reactor, Polyimide PI2545

Figure 4.7. Comparison of Standard and Electron Beam Exposed Samples in  $CF_4/O_2$  Plasma - Experiment 2



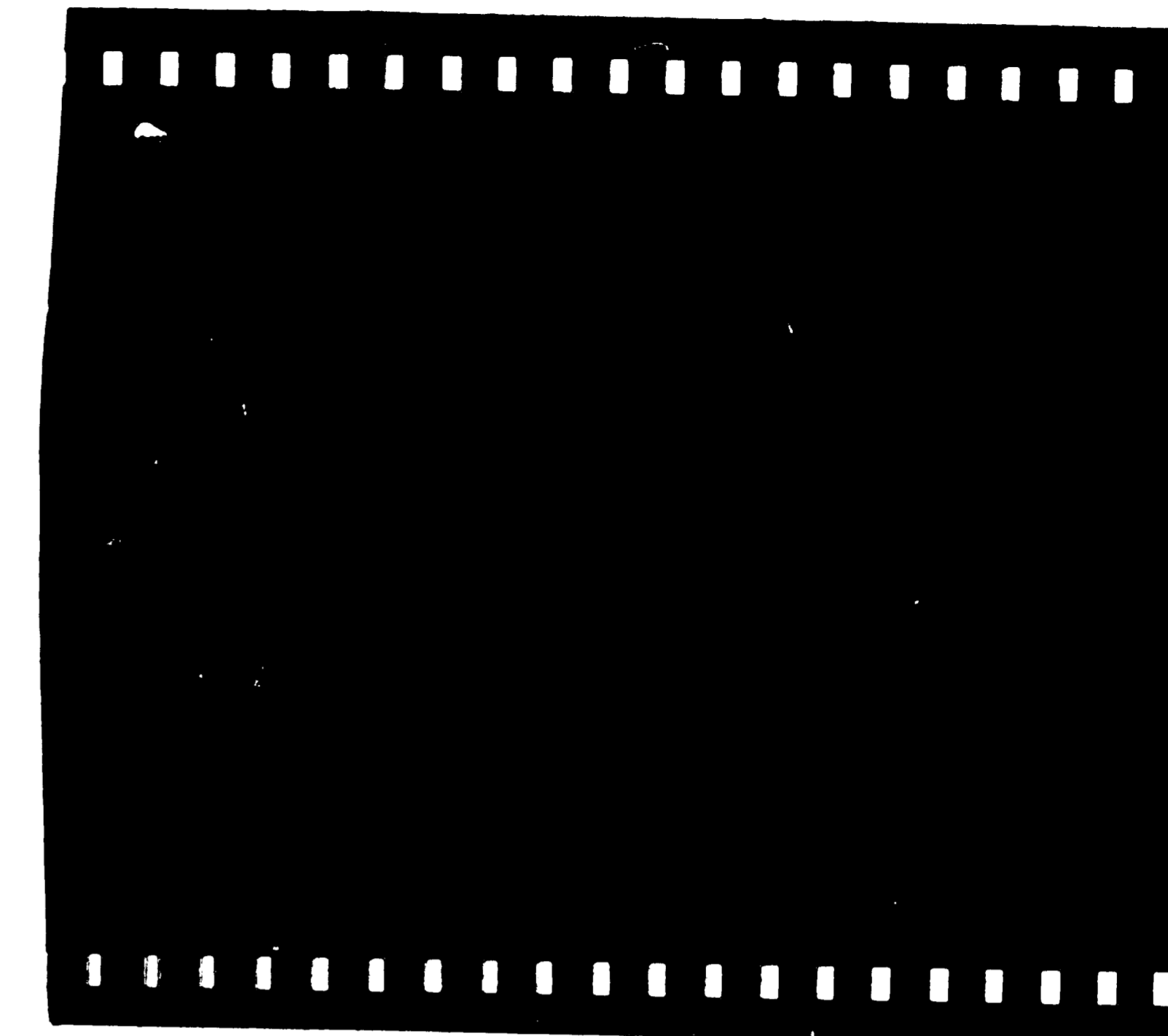
Step Measurement (Angstroms)

Sample Code	<u>Standard IR Cure</u>			<u>Electron Beam</u>		
	Position 1	Position 2	Position 3	Position 1	Position 2	Position 3
A2545	4450	3350	4000	2450	2500	2750
B2545	3000	3700	3950	3850	3100	3700
A2555	3850	3100	4100	2350	3600	4350
B2555	2500	1850	2000	3100	2750	2100
A2566	3750	3100	3350	5850	6700	7200
B2566	4870	5500	4750	3850	3950	3500

Coding Example: A2545 - Position A in reactor, Polyimide  
PI2545

Figure 4.8. Comparison of Standard and Electron Beam Exposed Samples in  $NF_3/O_2$  Plasma - Experiment 2

Standard



Electron Beam Exposed

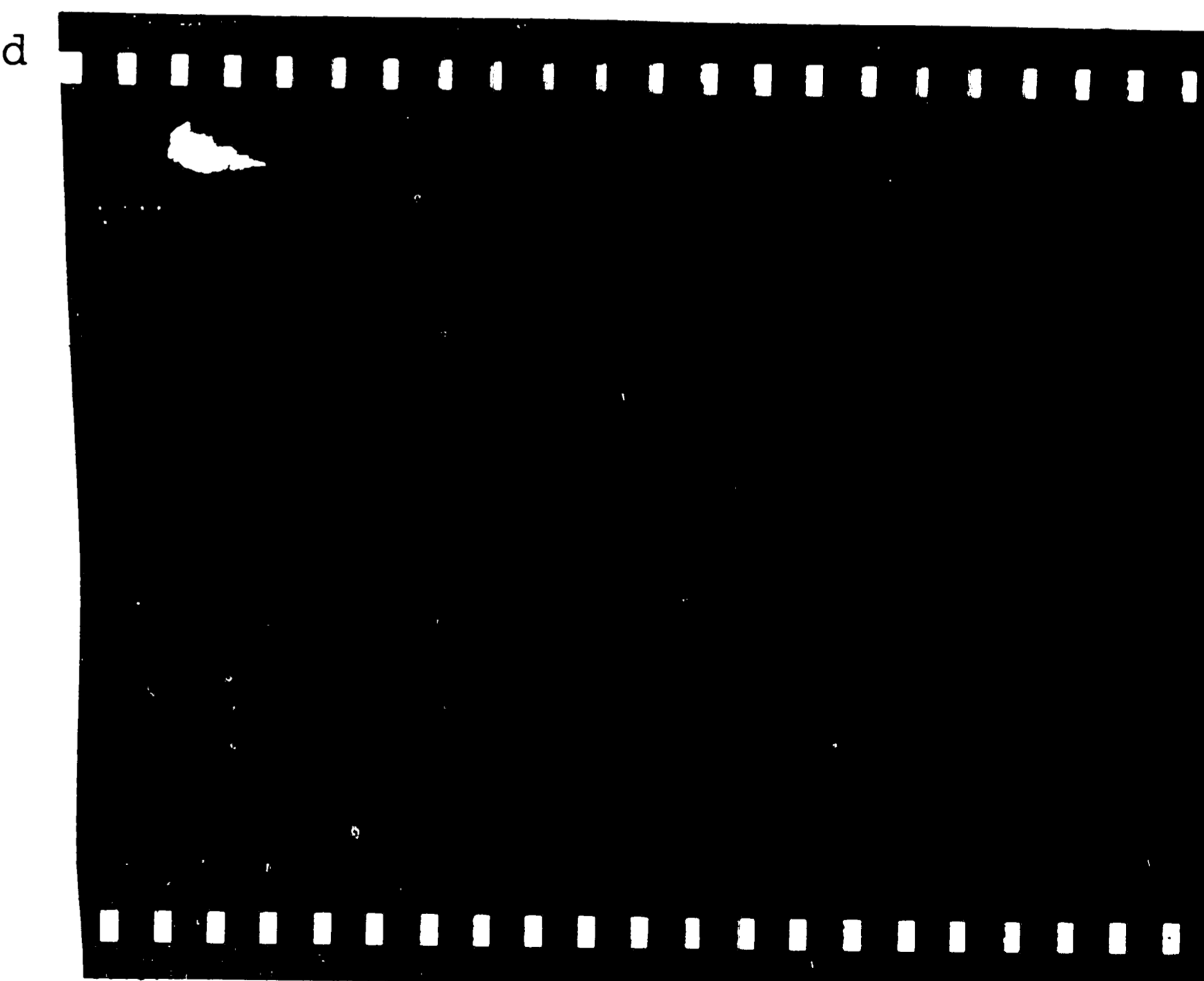


Figure 4.9. Samples of Electron Beam and Standard Polyimide Talysurf Traces for  $NF_3/O_2$  Plasma System

Step Measurement (Angstroms)

The following table shows the results of the step measurement of the surface of the specimen. The values are given in Angstroms. The surface is generally smooth, with a few small steps. The maximum step height is approximately 10 Angstroms. The surface roughness is very low, indicating a high quality of the specimen.

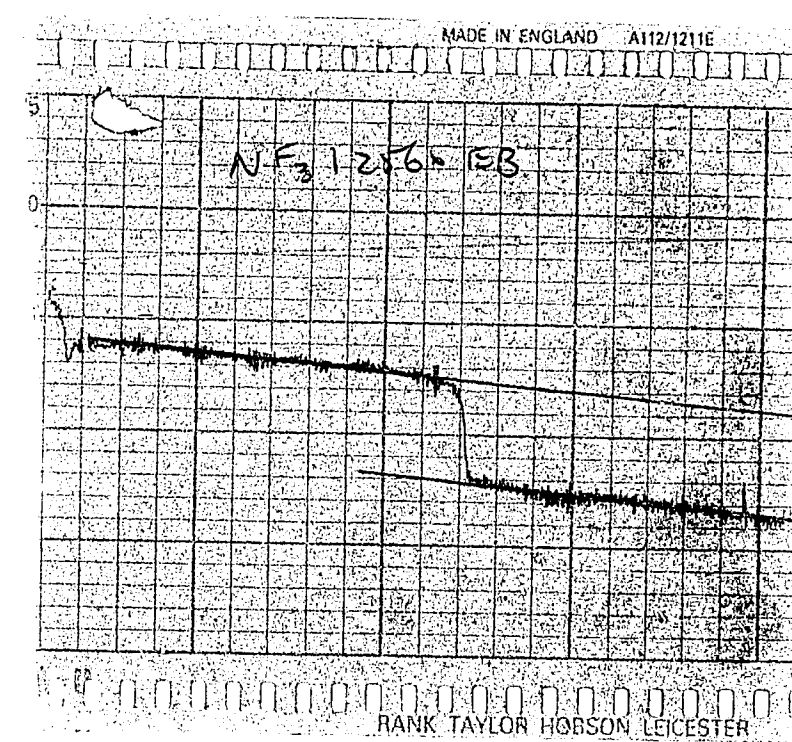
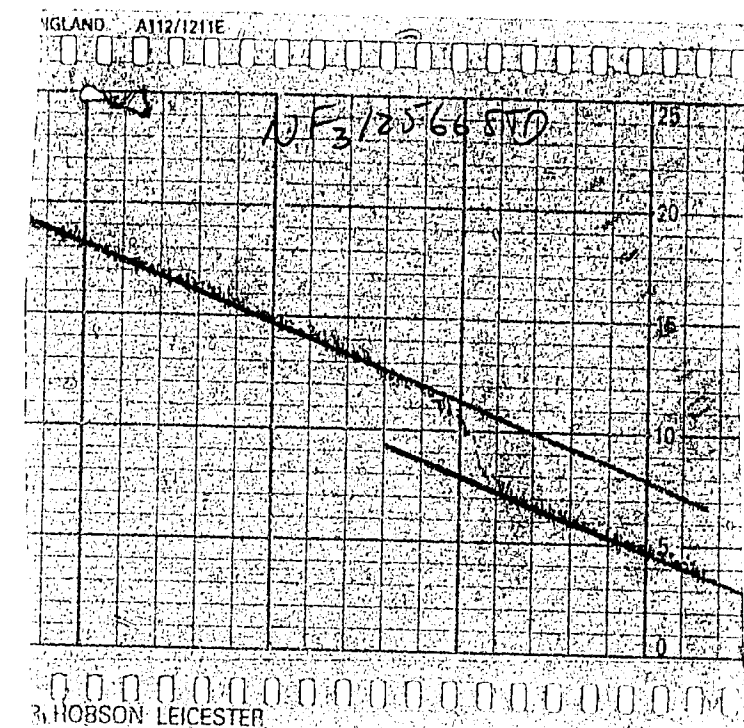
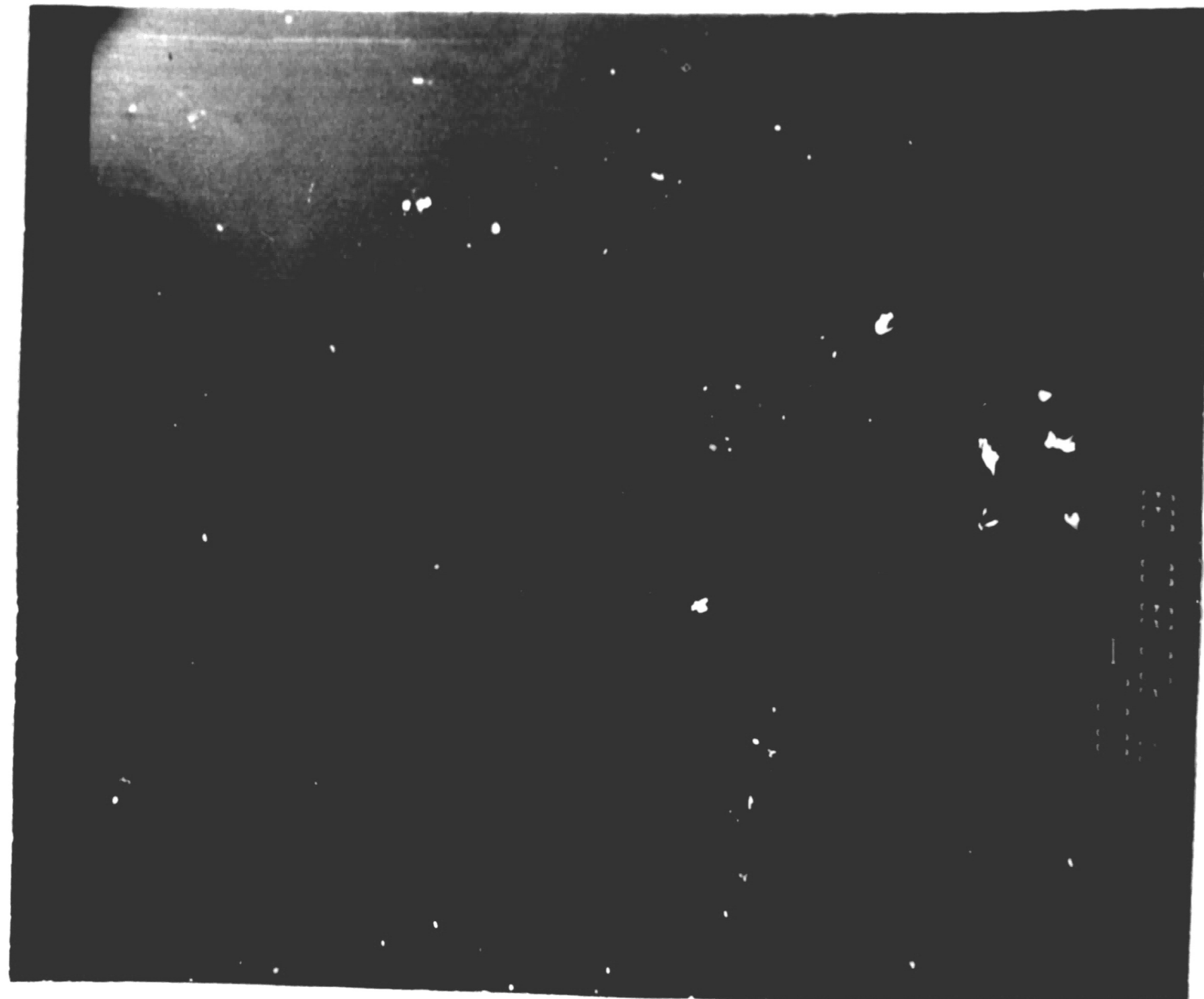


Figure 1. Comparison of the two surfaces and standard roughness measurements for NF<sub>3</sub>/O<sub>2</sub> Plasma system.

NFA2566  
Standard



NFA2566  
E-Beam  
Exposed

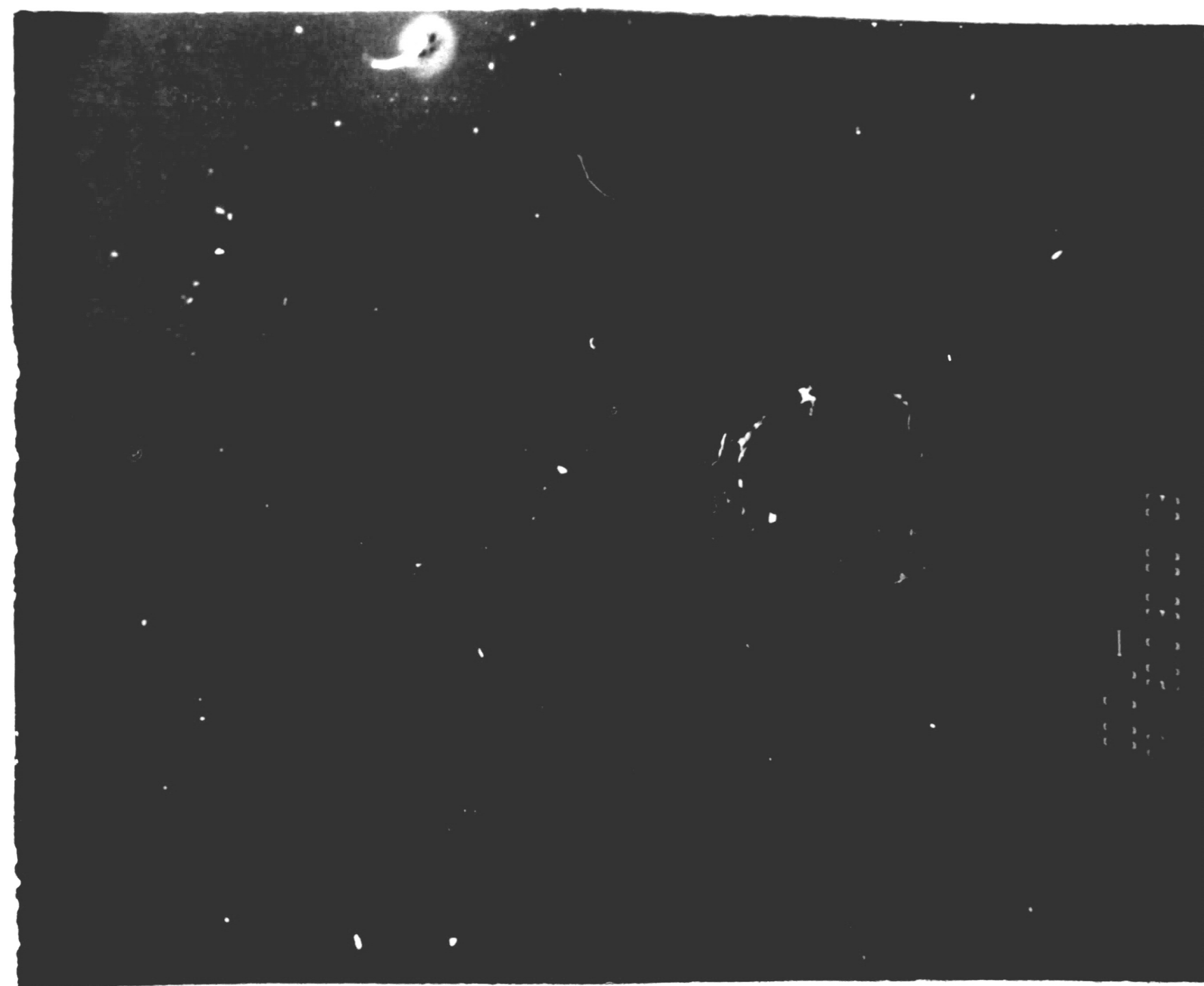
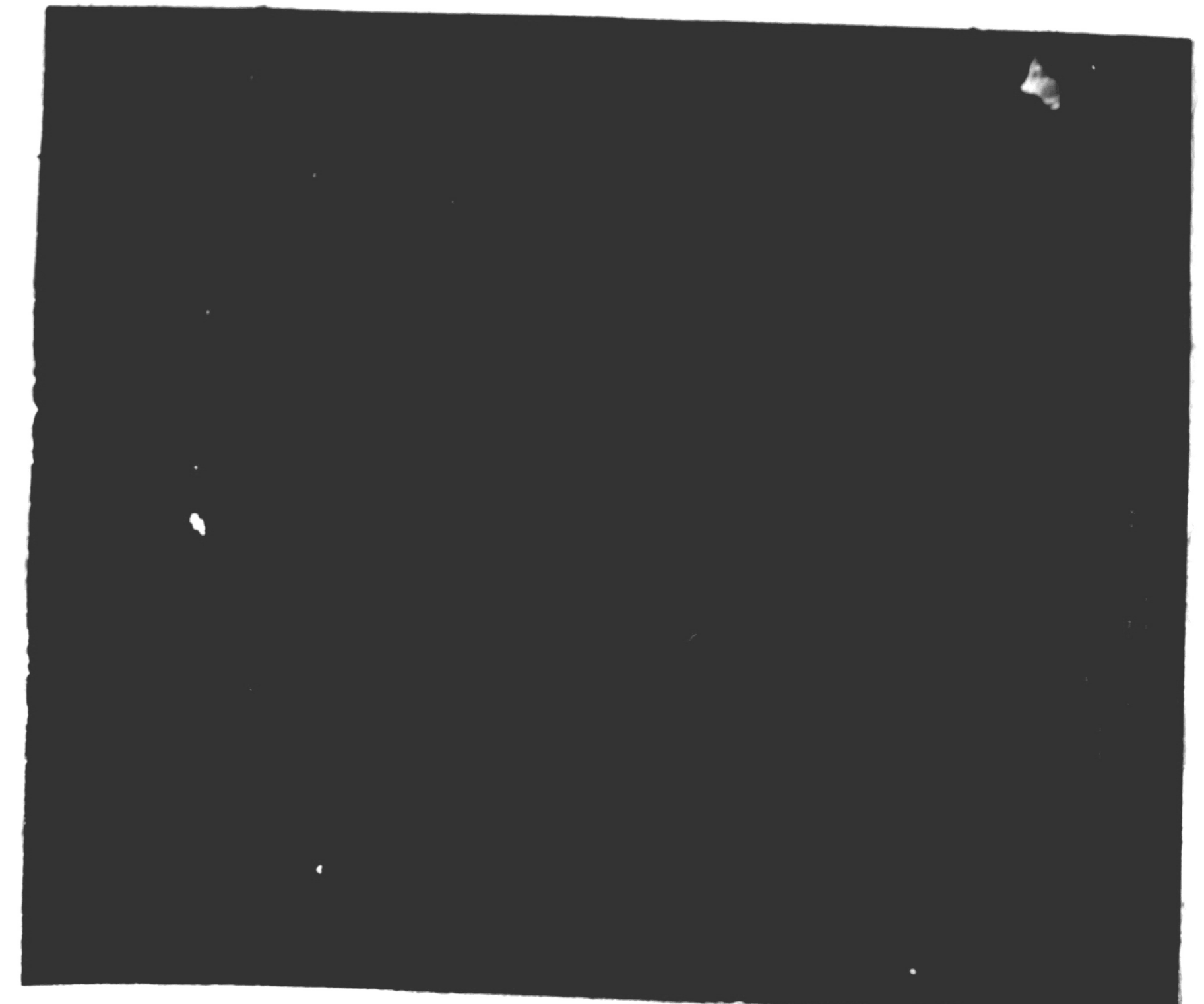


Figure 4.10. Photomicrographs of Samples NF12566 STD,  
NF12566 EB at 20X

NFA2566  
Standard

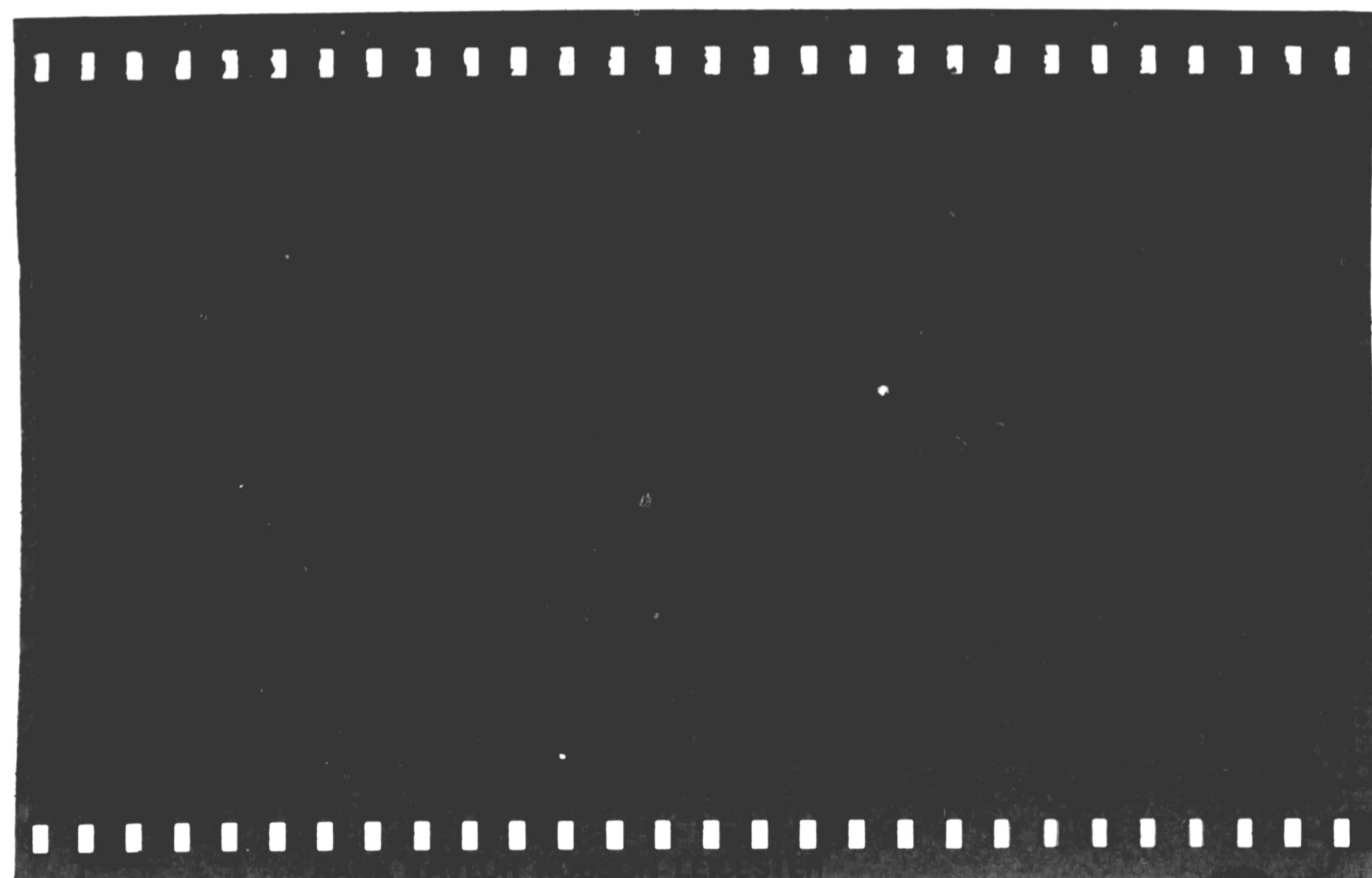


NFA2566  
E-Beam  
Exposed



Figure 4.11. Photomicrographs of Samples NF12566 STD,  
NF12566 EB at 200X

5000x



20,000x

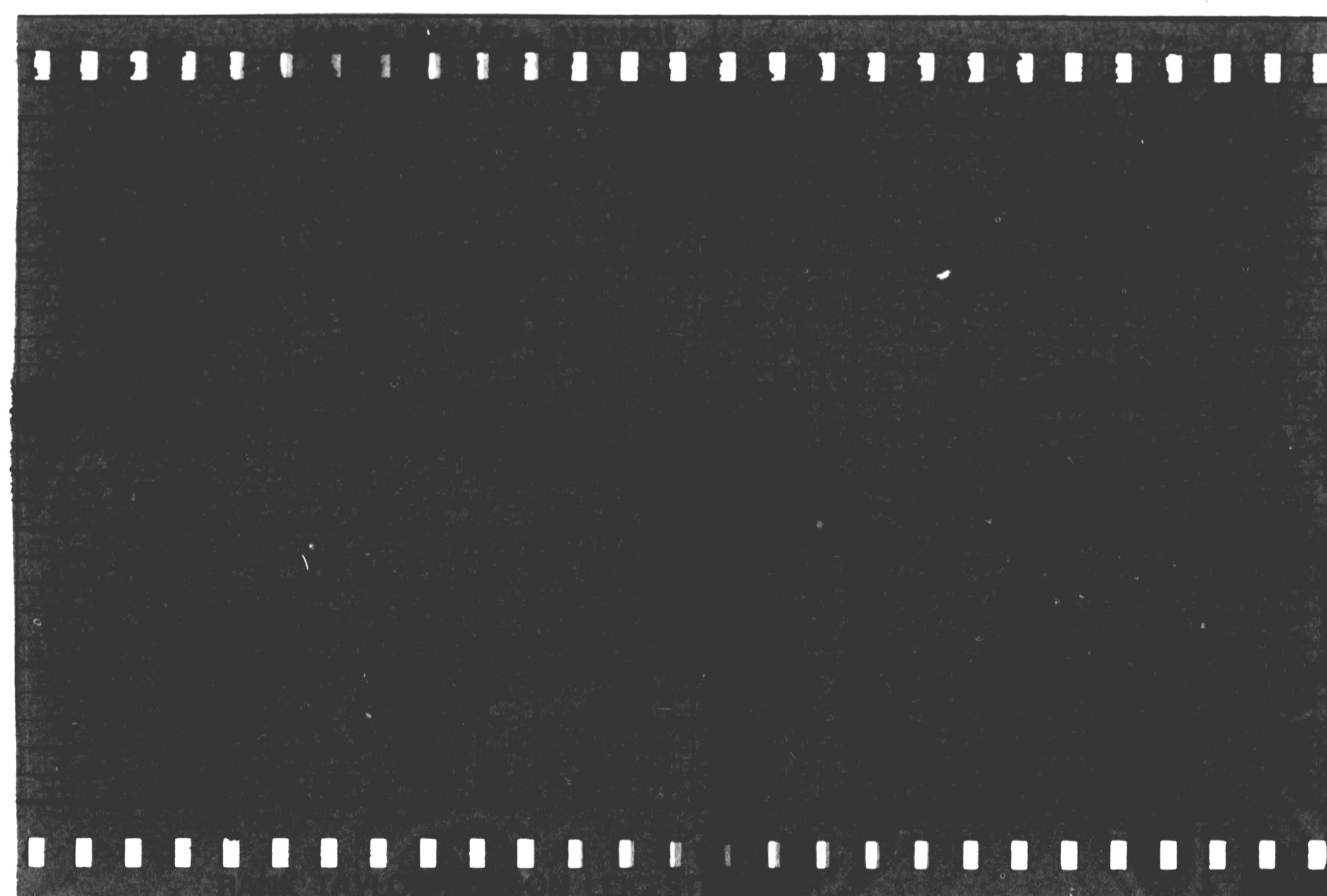
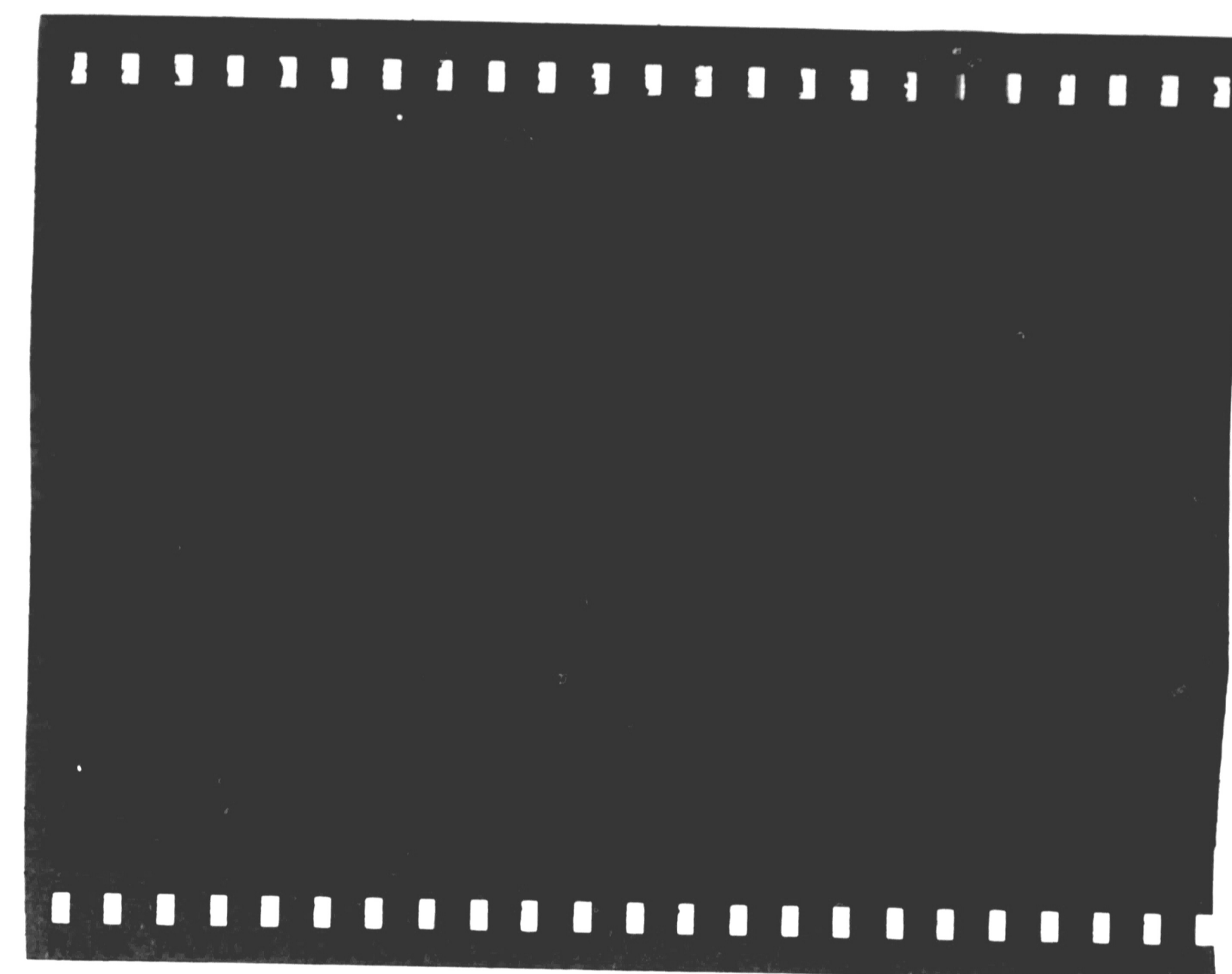


Figure 4.12. Talysurf Traces for PI-2566 at 5000x and 20,000x

5000x



20,000x

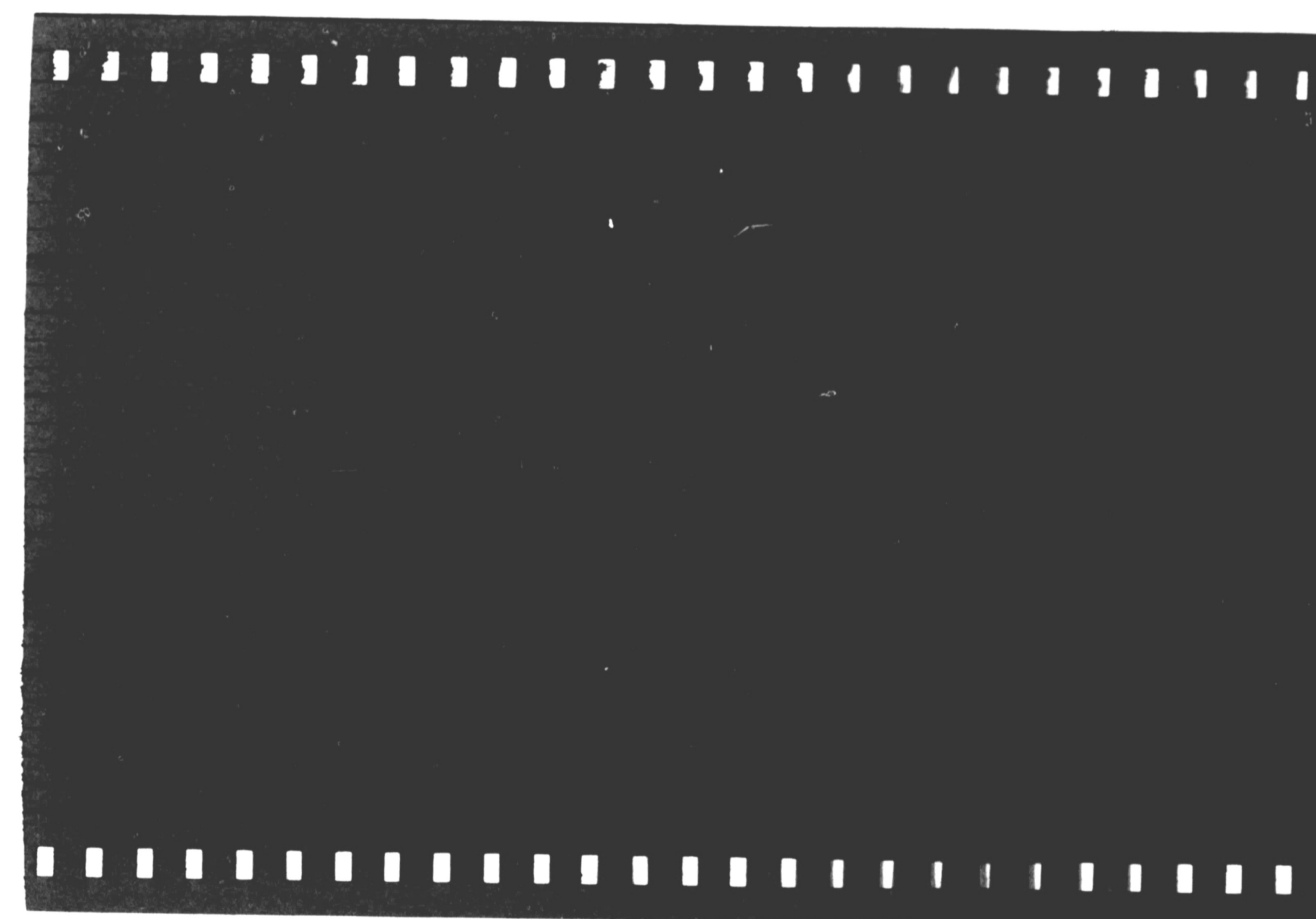
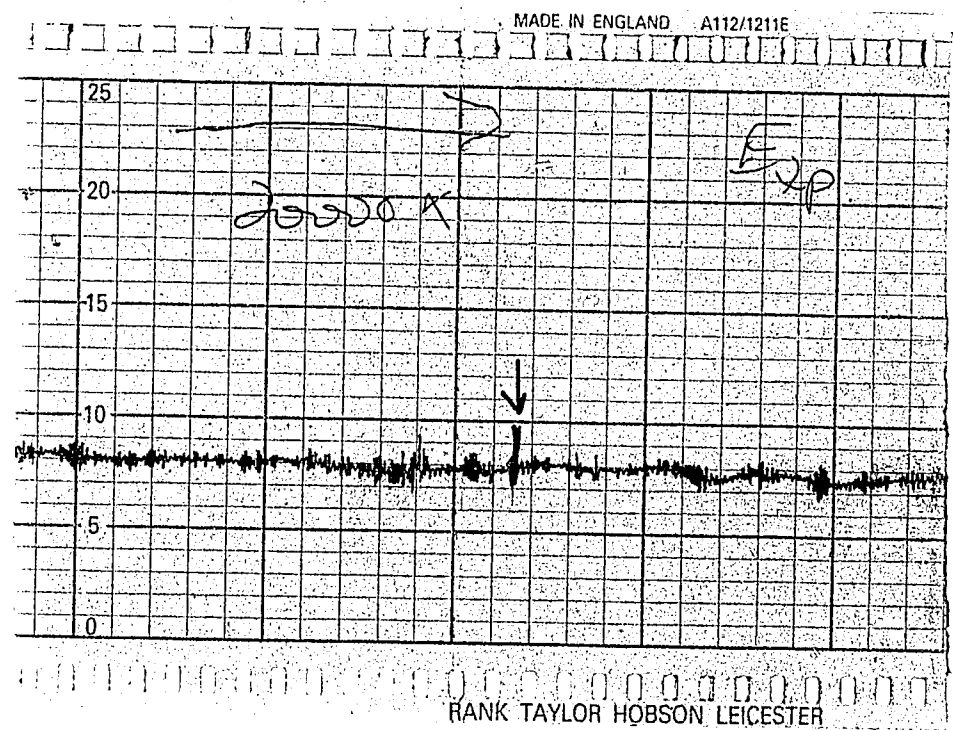
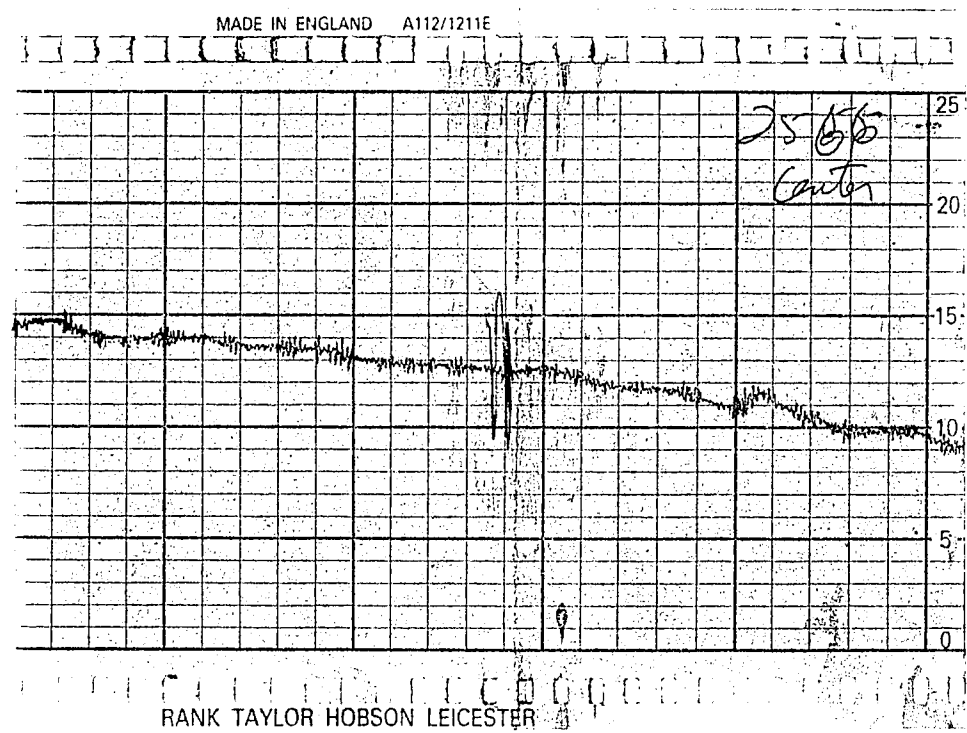
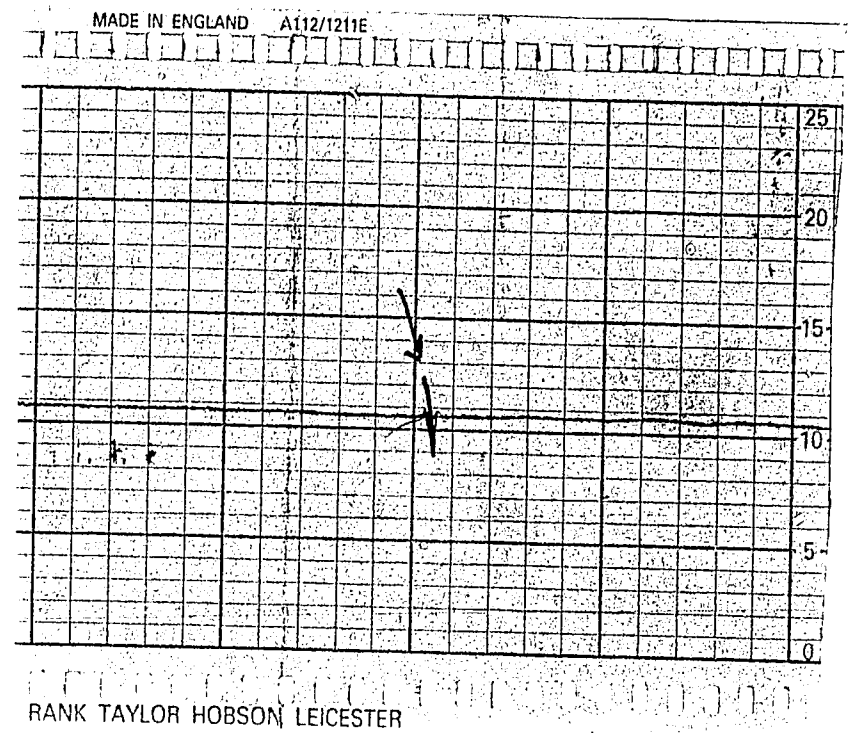
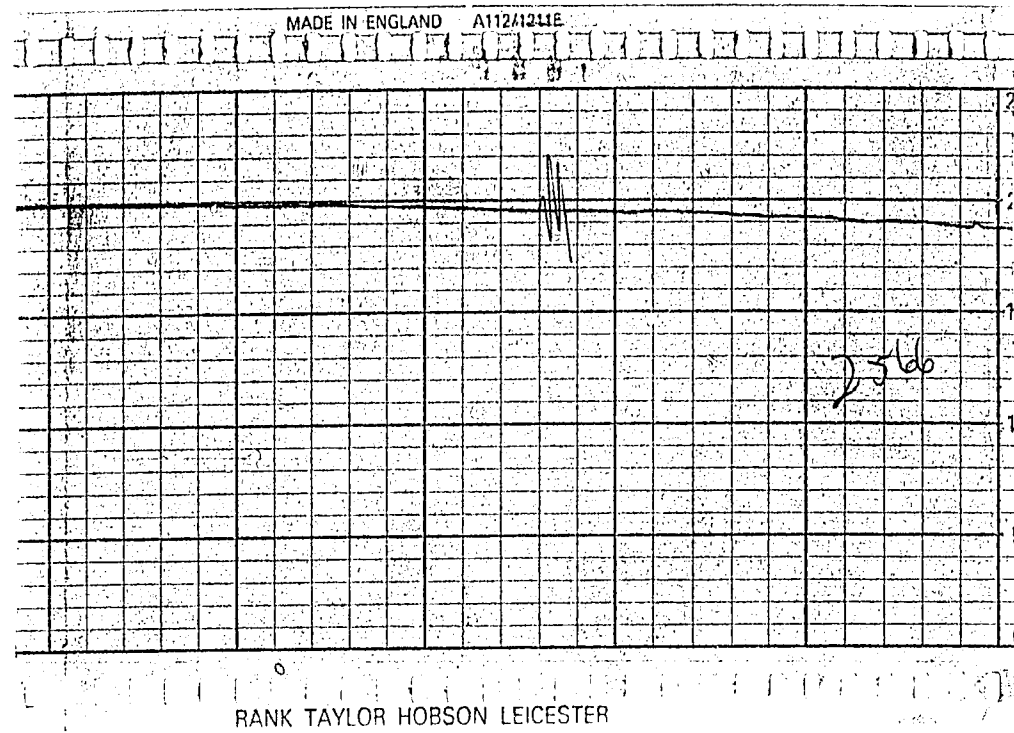


Figure 4.13. Talysurf Traces for PI-2555 at 5000 and 20,000x





## 5.0 Discussion

This work represents the initial attempt to assess the role of various excitations (UV, electron, X-ray) on the modification of the etch rate of polymers, in this case polyimide. As such, a great deal of the effort is involved in surveying suitable samples that were subjected to different radiations, and exploring for first order effects. The survey doses for the radiation were those that involved using local equipment and sample holders. In addition, a comparison of  $\text{NF}_3/\text{O}_2$  and  $\text{CF}_4/\text{O}_2$  etching was undertaken; not from a quantitative point of view but to assess whether either of these systems makes a large difference on the abruptness of the step height across masked and unmasked regions. The principle data then was the step height across the masked region on samples placed in two different locations, A and B, in the plasma reactor. The relative steepness of this interface represents the profile etched into the polymer. Since the survey experiments were carried out with a limited number of samples, only general trends could be ascertained. In addition, the variability in etching as a function of reactor position played a larger role than was initially assessed.

It can be seen in the data that within any one position in the reactor the  $\text{NF}_3/\text{O}_2$  system resulted in the

steepest profile in the samples with the lowest dose radiation representing, in general the steepest profile. In assessing the role of various excitations on etch rate, both the UV and X-ray samples resulted in the steepest profiles when subjected to etching in  $\text{NF}_3/\text{O}_2$  with the lowest dose samples showing the largest difference. No doubt that these preliminary results should be systematized in a future study of the influence of exposure dose on etch rate. Electron beam exposed samples tended to lower the etch rate of the polyimides in both gaseous etching systems, perhaps because of the measure of additional cross linking that occurs as a result of the bombardment. It is clear from the SEM photomicrographs of these samples that local area attack was important as seen by the circular patterns on these samples. This phenomenon should be an area of future investigation.

## 5.1 Step Measurements

The step profiles of some of the samples were not possible to measure, because the etch profile was not found under the microscope. The smallest profile found under magnification was 1583 angstroms found in Figure 4.5. The assumption has been made that those etch profiles not found under in the Dektak microscope were less than 1500 angstroms in step height.

Figures 4.2 - 4.5 show that the rate of etching

standard IR cured 5878 polyimide and radiation treated 5878 ranges from 600 - 1675 A/min. The measurements show a high variability between samples "A" and "B", in the same reactor run, as well as variability in thickness to a significant extent within the same sample readings. These variabilities can be attributed to different irregularities including the interpretation of the Dektak digital screen and the placement of the "R" and "M" cursors, plasma etch uniformity, and polyimide local irregularities in thickness.

With these variabilities in etch rates within the sample in mind, averaging the three data points to arrive at an etching rate for a specific treatment and reactant gas is not feasible. Instead, the numbers represented in the figure are averages of two locally close readings, in the positions mentioned earlier. In general then, some trends in the data were used to justify and narrow the scope of further experimentation for verification.

First, a comparison of the data values and high incidence of missing measurements in Figure 4.5 with the rest of the data suggests that the polyimide etch rate is lower for films exposed to the electron beam. Although there is evidence of equally low readings in other exposure categories, the consistency of the low readings, and the number of steps not found through the Dektak

microscope. in Figure 4.5 make this a viable trend for further examination.

Second, among the other exposures UV light and X-rays both appear to have sufficiently different step measurements as a function of exposure. I suggest that the possibility of a correlation for further study in these two areas should be pursued, but with attention to absolute dose and dose rate.

A third trend is the etch rate of the  $\text{NF}_3/\text{O}_2$  system vs the  $\text{CF}_4/\text{O}_2$  system. The etch rates, with some exceptions, appear to be 50% higher for the  $\text{NF}_3$  system.

The second experiment concentrated on these three characteristics of polyimide etching. Figures 4.7 and 4.8 give the results for a 10 minute etch on three different DuPont polyimides, trying to verify the weak trend found above on different polyimide formulations.

The use of the Talysurf in this application was necessary due to unavailability of the other instrument. The Talysurf has some drawbacks; no digital step measurement, no automatic leveling feature, and no on-line magnification capability. But, the Talysurf does produce an analog output of the trace, and is not limited by the size of the screen for reproduction of an undercut trend or roughness evaluation at areas far removed (2-4 mm) from the step.

The results were mixed. Some of the polyimide pairs, for example B2566 in both figures and A2545 in Figure 4.7 confirm the trend of approximately 50% greater etch rate for unexposed polyimide. Others, such as A2566 in Figure 4.8 deny the relationship. The question of differences in the rate measurement are related to the variables as before, but in this set, also related to interpretation of the Talysurf profile. Figure 4.6 illustrates the steps necessary for reading the thickness of the step on the Talysurf chart paper.

An examination of Figures 4.7 and 4.8 also shows that the difference in the etch rates found between polyimide formulations differ. Since these are proprietary films, a relation to formulation differences was not possible.

One last observation can be made from Figures 4.7 and 4.8. The etch rate difference found in the first experiment between the  $\text{NF}_3$  and  $\text{CF}_4$  chemistries, appears to not have held up. The rates are also much lower than the original experiment, since the etching time was twice that of experiment 1.

## 5.2 Profile Shape

The traces did provide additional insight by showing a small difference on the profiles with and without electron radiation. On approximately 40% of the traces

for  $\text{NF}_3$ , as shown in Figure 4.9, undercutting beneath the glass slide was more prevalent for exposed polyimide than for unexposed. This may represent a "hardening" or extended curing due to the beam, resulting in a straighter edge profile, and less mask undercut. The difference in the  $\text{NF}_3$  and  $\text{CF}_4$  systems and the relative amounts of undercutting seen is explained through the chemical nature of the  $\text{NF}_3$  etch, and the physical nature of the  $\text{CF}_4$  etch. The glass is a poor mask, because the fit is not nearly as good as, say, sputtered aluminum, but the difference in the under cut degree illustrates the chemical-physical biases of each process.

The SEM photomicrographs do not bear out the degree of undercut that can be interpreted from the Talysurf traces. The misleading factor in a Talysurf trace is the magnification factor (in this case 20X) used on the horizontal axis to provide information that stresses, or elongates the area of interest. The SEM photomicrograph in Figure 4.10 shows the etch line, the darker side was covered by the glass slide mask. However, repeated attempts to find a definitive step were not successful. The step appears to be much more gradual than the Talysurf tracings show. The reason is directly related to the masking technique used, and the lack of intimate contact with the substrate.

One interesting observation can be made, however, in Figure 4.11. At the 200X magnification, the surface of the unexposed sample appeared very smooth, and with no particular structure. The electron beam exposed sample on the other hand shows a circular type of defect in the polymer structure. The electron beam has had an obvious effect on the polyimide, but, as the step data point out, the effect on etch rate is not discernable in this experiment. Samples of this polyimide exposed to the electron beam were submitted for composition analysis, but were not complete at the time of this paper.

The findings in Experiment 2 were scattered enough to try a definitive test for etch rate variations. The preparation of the lead shield and exposure to the electron beam of half the sample resulted in no difference in etch rate of the two sides, when exposed to the more vigorous etchant,  $\text{NF}_3/\text{O}_2$ . Figures 4.10 and 4.11 present Talysurf traces at magnifications of 5000x and 20,000x. The top trace at 5000x gives a profile of the wafer that details the curvature in a macroscopic way. When the magnification is increased to 20,000x, the curvature can be interpreted with the more magnified profile.

The hash mark in each of the charts is where the profile needle crossed from the exposed to shielded (or vice versa) side. There is no indication, especially with

the 5000x trace as a reference, to believe that the exposure of the polyimides to the electron beam caused any change in etch rate.

### 5.3 Implications

This study appears to have raised more questions than it has answered. The etching of polyimide is a valuable process in the electronics industry, as mentioned in the introduction. The environments that materials must survive in are becoming more and more demanding. Polyimide appears to be a suitable material for such demanding applications. The data of this study support yet another attribute of polyimide, its ability to withstand radiation and electron bombardment with regard to effects on the etch rate. The restructuring of the film was obvious from the SEM photomicrographs.

The tailoring of an etch profile through a mask is another application of this study. With further research, if it can be determined that the shape of etched polyimide can be made perpendicular by a selection of electron exposures and plasma chemistry, fine line detail may be possible, and polyimide could be used as the patterning material, in a "permanent" type of resist configuration. The electrical properties of polyimide make it a candidate for this application, since interference can be reduced in

fine line geometries, and the film is durable enough to withstand processing, radiation, and the elements.

## 6.0 Summary of Conclusions

The following conclusions can be drawn from this study of etching radiation treated polyimides:

- 1 - The etch rate does not change appreciably when polyimide is exposed to electron beam, X-ray or UV radiation. The measurement techniques used provided for more work and doubt than a laser interferometry system that measures etch rates in situ would have.
- 2 - Undercutting was present in untreated samples, although the degree is somewhat mismatched between the SEM and Talysurf analysis. The chemical nature of the  $\text{NF}_3$  plasma is illustrated in this application.
- 3 - The etch rate of the polyimides ranged from 600 - 1675 A/min. A high degree of variability was found both from sample to sample and within the same sample.
- 4 - Polyimide's etch rate is much lower than that of photoresist, where the etch rate can be as high as 10,000 A/min for the  $\text{NF}_3$  concentration used in this study.
- 5 - Electron beam radiation did cause damage to the polyimide, although this transition is unknown, and did not effect the etch rate.

### 7.0 Recommendations for Future Research

The following research topics would compliment this preliminary study, and provide answers to the many questions generated:

- 1 - The effect of electron beam radiation in tailoring the sidewalls of the profile have been suggested. A further study of this effect, its degree of anisotropy, and the effect of variable radiation doses on the shape of the profile could be considered.
- 2 - An applied research project using polyimide as the patterning mask could be done to investigate the resolution of the plasma patterning technique.
- 3 - A follow up investigation could be done to study the resolution of radiated and standard polyimide patterned circuits.
- 4 - The concept of exposing polyimide to environmental damage should be extended to include ion implantation.

- 5 - Surface analyses of electron beam and X-ray exposed polyimide would determine specifically what the effects reported in this thesis are regarding electron beam exposed polyimide. The circular patterns noted in the SEM photomicrographs are interesting from a point of structure after radiation.

## References

- [1] S.J. Fonash, "Advances in Dry Etching Processes - A Review," Solid State Technology, January 1985, p. 150
- [2] J.W. Coburn and H.F. Winters, "Plasma Etching - A Discussion of Mechanisms," Journal of Vacuum Science and Technology B, Vol. 16, No. 2, p. 391, March/April 1979
- [3] H.F. Winters, "The Role of Chemisorption in Plasma Etching," Journal of Applied Physics, 49, 5165, 1978
- [4] J.E. Rowe, G. Margaritondo, and S.B. Christmas, "Chlorine Chemisorption on Silicon and Germanium Surfaces: Photoemission Effects with Synchrotron Radiation," Physical Review B, 16, 1581, 1977
- [5] K.C. Pendley, T. Sakurai, and H.D. Hagstrum, "Chemisorption of Chlorine on Si (111) 7X7 and 1X1 Surfaces," Physical Review B, 16, 3648, 1977
- [6] YY Tu, T.J. Chuang, and H.F. Winters, "Chemical Sputtering of Fluorinated Silicon," Physical Review B, 23, p. 823, 1981
- [7] C.J. Mogab and H.J. Levenstein, "Anisotropic Plasma Etching of Polysilicon," Journal of Vacuum Science and Technology, 17, 1980, p. 721
- [8] R.H. Bruce, "Anisotropy Control in Dry Etching," Solid State Technology, 24, p.64, October 1981
- [9] W.R. Harshbarger, R.A. Porter, T.A. Miller and P. Norton, "A Study of the Optical Emission from an rf Plasma During Semiconductor Etching," Applied Spectroscopy, 31, p. 201, 1977
- [10] F.D. Egitto, F. Emmi, and R.S. Horwath, "Plasma Etching of Organic Materials. I. Polyimide in O<sub>2</sub>-CF<sub>4</sub>," Journal of Vacuum Science and Technology B, 3(3) p. 893, May/June 1985
- [11] G. Turban and M. Rapeaux, "Dry Etching of Polyimide in O<sub>2</sub>-CF<sub>4</sub> and O<sub>2</sub>-SF<sub>6</sub> Plasmas," Journal of the Electrochemical Society, 130, p.2231, November 1983

- [12] T. Yogi, K. Saenger, S. Purushothaman, and C.P. Sun, "Polyimide Etching in O<sub>2</sub>/CF<sub>4</sub> RF Plasmas," Proceedings of the Electrochemical Society, 85-1, p. 216, 1985
- [13] D.S. O'Grady, "Etching of Polymers in a NF<sub>3</sub>/O<sub>2</sub> Plasma," Master's Degree Thesis, Lehigh University, 1986
- [14] J.A. Barkanic, D.M. Bohling, D.M. Reynolds, "A Review and Safety Considerations of Dry Etching Using Nitrogen Trifluoride," Air Products and Chemicals Inc., Ref. 5039F-V2
- [15] R. Sellamuthu, J. Barkanic, and R. Jaccodine, "Anisotropic Trench Etching of Si with NF<sub>3</sub>-Halocarbon Mixtures," Tegal 12<sup>th</sup> Plasma Seminar, May 1986
- [16] N.A. Adrova, M.I. Bessonov, L.A. Laius, and A.P. Rudakov, Polyimides - A New Class of Heat Resistant Polymers, Academy of Sciences of the USSR, Institute for High Molecular Compounds, Leningrad, USSR, 1968 p.4
- [17] Ibid. p. 65
- [18] V. Shrinet, U.K. Chaturvedi, S.K. Agrawal, V.N. Rai, and A.K. Nigam, "Effect of Neutron and Proton Irradiation on Some Properties of Kapton," Polyimides - Synthesis, Characterization and Applications, Edited by K.L. Mittal, Plenum Press, New York, New York, 1984, p. 555
- [19] L.B. Rothman, "Properties of Thin Polyimide Films," Journal of the Electrochemical Society, 127, p. 2216, October 1980



### Vita

Eric Dibble was born in Syracuse NY on March 31, 1959 to Margaret and Ronald Dibble. He attended Union Endicott High School in Endicott, NY where he graduated with honors in 1977. He graduated from Clarkson College of Technology in May 1981 with a B.S. in chemical engineering.

He started with IBM Corporation in Endicott, NY in June of 1981 as an associate engineer in precious metal plating equipment and process development. Major assignments included development of equipment and processes for the 9370 computer circuit card connections.

In August of 1985 Eric entered the IBM sponsored Manufacturing Systems Engineering (MSE) program at Lehigh.

### Abstract

Title: Etching Radiation Treated Polyimide Films in  $O_2/NF_3$  and  $O_2/CF_4$  Plasmas

Author: Eric P. Dibble

Advisor: Ralph J. Jaccodine

The effect of radiation on the etch rate of polyimide in  $NF_3/O_2$  and  $CF_4/O_2$  plasmas has been studied. Polyimide samples have been exposed to UV light, X-rays and electron beam radiation. The etch rate and profile of a step generated in the polyimide by a glass plate mask during etching have been investigated to determine the effect of the radiation.

Problems occurred in trying to reproduce step measurements, due to the variability of the measurement instruments, and the plasma reactor etch profile. A high degree of variability was observed both from sample to sample and within the same sample. A final experiment produced both a standard IR cured sample and an electron beam exposed sample on the same specimen, and a final determination of degree of etch was made.

Radiation from the mentioned sources produced no effect on the etch rate of the polyimide. The final set of samples mentioned showed no step where the exposed/unexposed boundary was crossed. A slight effect was noticed in the film step profile with the electron

beam radiation. Undercutting appeared to be less with the radiated samples, compared to the standards. SEM photomicrographs show damage was produced by the electron beam, but the damage does not produce etch rate changes.